Power System Harmonics and Passive Filter Designs

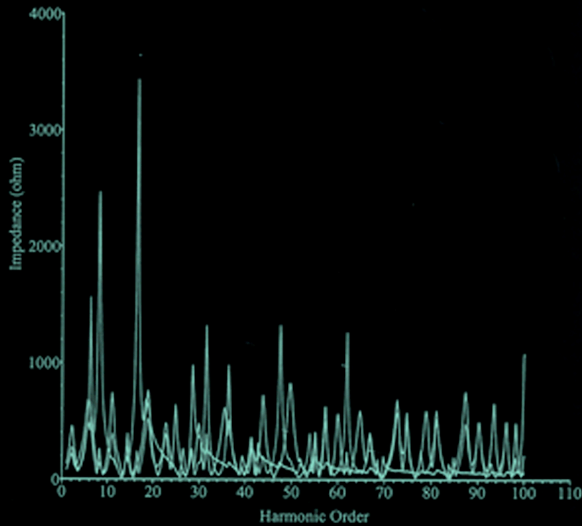

J.C. Das

IEEE
IEEE PRESS

IEEE PRESS SERIES ON POWER ENGINEERING
Mohamed E. El-Hawary, *Series Editor*

WILEY

POWER SYSTEM HARMONICS AND PASSIVE FILTER DESIGNS

POWER SYSTEM HARMONICS AND PASSIVE FILTER DESIGNS

J.C. DAS

IEEE PRESS SERIES ON POWER ENGINEERING

IEEE PRESS

WILEY

Published by John Wiley & Sons, Inc., Hoboken, New Jersey.
Published simultaneously in Canada

Library of Congress Cataloging-in-Publication Data:

Das, J. C., 1934-
Power system harmonics and passive filter design / J. C. Das.
pages cm
ISBN 978-1-118-86162-2 (hardback)
1. Electric power system stability. 2. Harmonics (Electric waves) 3. Electric filters, Passive. I. Title.
TK1010.D37 2015
621.31′7–dc23

2014034588

Printed in the United States of America

10 9 8 7 6 5 4 3 2 1

CONTENTS

CHAPTER 7 *ESTIMATION AND MEASUREMENTS OF HARMONICS* 281

CHAPTER 8 *EFFECTS OF HARMONICS* 331

FOREWORD

***Dr. Jean Mahseredjian*[1]**

This book on power system harmonics and passive filter designs is a comprehensive resource on this subject, covering harmonic generation, mitigation, measurement and estimation, limitations according to IEEE and IEC standards, harmonic resonance, formation of shunt capacitor banks, modeling of power system components and systems. Harmonic penetration in the power systems, passive filters, and typical study cases, covering renewable energy sources – solar and wind power generation – are included. There are many aspects of harmonics discussed in this book, which are not covered in the current publications.

The following is a chapter-wise summary of the book content.

Chapter 1 forms a background on the subject of power system harmonics with discussions of harmonic indices and power theories. The coverage of nonsinusoidal single-phase and three-phase systems and popular instantaneous power theory of H. Akagi and A. Nabe, much used for active filter designs discussed later on in the book, leads a reader to understand the nonlinearity.

The second chapter on Fourier analysis, though much mathematical, paves the way for the applications to harmonic analysis and measurements with limitations of window functions. The examples given in the chapter help the readers to understand the transformations.

Harmonic generation from conventional power equipment, ferroresonance, and electronically switched devices, converters, home appliances, cycloconverters, PWM, voltage source converters, switch mode power supplies, wind farm generation, pulse burst modulation, chopper circuits, traction and slip recovery schemes, are well described in Chapters 3 and 4. A reader will find an interesting analysis of transformer modeling, third harmonic voltages in generators, and many EMTP simulations. Harmonics due to saturation of current transformers is an added feature. Chapter 4 is fairly exhaustive and includes harmonic generation from many sources of practical importance. The analysis and topologies of ASDs (adjustable speed drives) are well documented. Though the author provides some background, yet a reader must be conversant with elements of power electronics.

Interharmonics is a new field of research, and Chapter 5 is well written so as to provide a reader a clear concept of interharmonic generation and their effects. This is followed by a well-written work on flicker from arcing loads, arcing and induction

[1]Dr. Jean Mahseredjian is an IEEE-Fellow and Professor of Electrical Engineering at École Polytechnique de Montréal, Montréal, Québec, Canada. He is world renowned authority on the simulation and analysis of electromagnetic transients. He was also a member of IEEE working groups on Power System Harmonics.

furnaces, and tracing methods of flicker. The control of flicker through the application of a STATCOM followed by torsional analysis due to harmonics in large drives with graphics is one problem that is not so well addressed in current texts. The subsynchronous resonance in series compensated HV transmission lines and drive system cascades, with EMTP simulation results, will be of interest to special readers interested in this field.

Having discussed the generation of harmonics in previous chapters, Chapter 6 is logically placed to discuss the various strategies that can be adopted to reduce the harmonics at source itself, so that harmonic penetration in the power systems is avoided. This covers active filters, combination of active and passive filters, their controls, active current shaping matrix converters, multilevel inverters, THMI inverters and theory of harmonic reduction at source, new breed of matrix and multilevel converters, followed with the theory of the resultant of polynomials. Then, the demonstration of this theory and control of switching angles is demonstrated to reduce harmonic distortion to a very low level. Some sections of this chapter will need a prior understanding of many aspects of converters and their switching, and on first reading the mathematical treatment cannot be easily followed by an average reader. The author provides excellent references at each step for further reading.

The calculations, estimation, time stamp of harmonics are the first step before a model can be generated for study. The relevance of modeling angles of the harmonics, measuring equipment, transducers, analysis of various waveforms will be of interest to all readers, while probabilistic concepts, regression methods, Kalman filtering, and so on will be of special interest. The author provides fundamental aspects leading to these advanced concepts.

The effects of harmonics can be very deleterious on electrical power equipment, Chapter 8. Practically all power system equipment of interest, motors, insulation stresses, and traveling wave phenomena on drive system cables, common mode voltages, bearing currents, protective relaying, circuit breakers, and the like are covered. Of special interest to a reader will be derating of dry and liquid-filled transformers serving nonlinear loads, which at times may be ignored, resulting in overloads.

After this background is grasped, harmonic resonance in various forms is discussed in Chapter 9. The reactance curves, Foster networks, composite resonance, secondary resonance are illustrated, which are commonly missing topics in other texts.

The limits of harmonic distortions in Chapter 10 cover both, IEEE and IEC guidelines, with limits on interharmonics and calculations of effects of notching on harmonic distortions.

In the design of passive filters, formation of shunt capacitor banks and their grounding and protection is an important aspect, Chapter 11. Often failures on harmonic filters occur due to improper selection of the ratings of unit capacitors forming the bank, as well as ignoring their protection and switching transients. The importance of this chapter cannot be overstated for a reader involved in harmonic filter designs.

The next step in harmonic analysis is accurate modeling of power system components and power systems, depending on their nature and extent of study, which is detailed in Chapters 12 and 13. These two chapters form the backbone of harmonic analysis. The modeling described for transmission lines, transformers, loads, cables, motors, generators, and converters in Chapter 12 is followed by system modeling in industrial, distribution, and transmission systems and HVDC, which are the aspects that should be clearly grasped by a reader interested in harmonics.

Study of harmonic penetration discussed in Chapter 14 can be undertaken after the material in the previous chapters is grasped. Apart from time and frequency domain methods, the chapter covers the latest aspects of probabilistic modeling.

It may seem that in the entire book only one chapter, Chapter 15, is devoted to passive filters. However, harmonic filter designs may be called the last link of the long chain of harmonic studies. The chapter describes practically all types of passive filters commonly applied in the industry, with some new technologies such as genetic algorithms and particle swarm theories.

Lastly, Chapter 16 has many real-world studies of harmonic analysis and filters designs, including arc furnaces, transmission systems, solar and wind generation plants. A reader with adequate modeling tools and software can duplicate these studies and it will be a tremendous exercise in learning.

I conclude that the book is well written and should appeal to beginners and advanced readers, in fact, this can become a standard reference book on harmonics. Many solved examples and real-world simulations of practical systems enhance the understanding. The book is well illustrated with relevant figures in each chapter.

PREFACE

The power system harmonics is a subject of continuous research; this book attempts to present the state-of-art technology and advancements. It is a subject of interest of many power system professionals engaged in harmonic analysis and mitigation and the applications in the modern climate when the nonlinear loads in the utility systems are on the increase.

The book provides a comprehensive coverage of generation, effects, and control of harmonics. New harmonic mitigation technologies, detailed step-by-step design of passive filters, interharmonics, and flicker are covered. The intention is that the book can serve as a reference and practical guide on harmonics.

A beginner should be able to form a clear base for understanding the subject of harmonics, and an advanced reader's interest should be simulated to explore further. A first reading of the book followed by a detailed critical reading is suggested. The many real-world study cases, examples, and graphics strive for this objective and provide clear understanding. The subject of harmonics may not form a curriculum even for graduate studies in many universities. In writing this book, an undergraduate level of knowledge is assumed; yet, the important aspects with respect to connectivity of each chapter are not lost sight of. It has the potentiality of serving as advance undergraduate and graduate textbook. Surely, it can serve as continuing education textbook and supplementary reading material.

The effects of harmonics can be experienced at a distance, and the effect on power system components is a dynamic and evolving field. These interactions have been analyzed in terms of current thinking.

The protective relaying has been called "an art and science." The author will not hesitate to call the passive harmonic filter designs and mitigation technologies the same. This is so because much subjectivity is involved. Leaving aside high-technology research tools such as Monte Carlo simulations, the available computer techniques invariably require iterative studies to meet a number of conflicting objectives.

A first reading of the book will indicate that the reader must understand the nature of harmonics, modeling of power system components, and characteristics of filters, before attempting a practical filter design for real-world applications. Chapter 16 is devoted to practical harmonic passive filter designs and case studies including solar and wind generation. A reader can modal and reproduce the results and get a "feel" of the complex iterative and analytical procedures.

The author acknowledges with thanks permission for republication of some work from his book: *Power System Analysis: Short-Circuit Load Flow and Harmonics*, CRC Press.

J.C. Das

ABOUT THE AUTHOR

J.C. Das is principal and consultant with Power System Studies, Inc. Snellville, Georgia. He headed the Power System Analysis department at AMEC, Inc. for many years. He has varied experience in the utility industry, industrial establishments, hydroelectric generation, and atomic energy. He is a specialist in performing power system studies, including short circuit, load flow, harmonics, stability, arc flash hazard, grounding, switching transients, and protective relaying. He conducts courses for continuing education in power systems and has authored or coauthored about 65 technical publications nationally and internationally. He is the author of the following books:

- *Arc Flash Hazard Analysis and Mitigation*, IEEE Press, 2012.
- *Transients in Electrical Systems: Analysis Recognition and Mitigation*, McGraw-Hill, 2010
- *Power System Analysis: Short-Circuit Load Flow and Harmonics, Second Edition*, CRC Press, 2011.

These books provide extensive converge, running into more than 2400 pages and are well received in the technical circles. His interests include power system transients, EMTP simulations, harmonics, power quality, protection, and relaying. He has published 200 study reports on electrical power system for his clients.

Related to harmonic analysis, Mr. Das has designed some large harmonic passive filters in the industry, which are in successful operation for more than 18 years.

Mr. Das is a Life Fellow of Institute of Electrical and Electronics Engineers, IEEE (United States), Member of the IEEE Industry Applications and IEEE Power Engineering societies, a Fellow of Institution of Engineering Technology (United Kingdom), a Life Fellow of the Institution of Engineers (India), a Member of the Federation of European Engineers (France), and a member of CIGRE (France). He is a registered Professional Engineer in the States of Georgia and Oklahoma, a Chartered Engineer (C. Eng.) in the United Kingdom and a European Engineer (Eur. Ing.) in the Europe. He received meritorious award in engineering, IEEE Pulp and Paper Industry in 2005.

He received MSEE degree from the Tulsa University, Tulsa, Oklahoma, and BA (advanced mathematics) and BEE degrees from the Punjab University, India.

CHAPTER 1

POWER SYSTEM HARMONICS

The electrical power systems should be designed not only for the sinusoidal currents and voltages but also for nonlinear and electronically switched loads. There has been an increase in such loads in the recent times, and these can introduce harmonic pollution, distort current and voltage waveforms, create resonances, increase the system losses, and reduce the useful life of the electrical equipment. Harmonics are one of the major problems of ensuring a certain power quality. This requires a careful analysis of harmonic generation and their measurements and the study of the deleterious effects, harmonic controls, and limitation to acceptable levels. Interest in harmonic analysis dates back to the early 1990s in connection with high voltage DC (HVDC) systems and static var compensators (SVC; Reference [1]). The analytical and harmonic limitation technology has progressed much during this period (see Reference [2] for a historical overview of the harmonics in power systems).

DC power is required for a number of applications from small amount of power for computers, video equipment, battery chargers, UPS (uninterrptible power supplies) systems to large chunks of power for electrolysis, DC drives, and the like. A greater percentage of office and commercial building loads are electronic in nature, which have DC as the internal operating voltage. Fuel and solar cells and batteries can be directly connected to a DC system, and the double conversion of power from DC to AC and then from AC to DC can be avoided. A case study conducted by Department of Electrical Power Engineering, Chalmers University of Technology, Gothenburg, Sweden is presented in [3]. This compares reliability, voltage drops, cable sizing, grounding and safety: AC verses DC distribution system. In Reference [4], DC shipboard distribution system envisaged by US Navy is discussed. Two steam turbine synchronous generators are connected to 7000 V DC bus through rectifiers, and DC loads are served through DC–DC converters. However, this is not a general trend, bulk and consumer power distribution systems are AC; and we will not be discussing industrial or commercial DC distribution systems in this book, except that HVDC converter interactions with respect to harmonics and DC filters are of interest and discussed in the appropriate chapters.

Harmonics in power systems originate due to varied operations, for example, ferroresonance, magnetic saturation, subsynchronous resonance, and nonlinear and electronically switched loads. Harmonic emission from nonlinear loads predominates.

Power System Harmonics and Passive Filter Designs, First Edition. J.C. Das.

1.1 NONLINEAR LOADS

To distinguish between linear and nonlinear loads, we may say that linear time-invariant loads are characterized so that an application of a sinusoidal voltage results in a sinusoidal flow of current. These loads display constant steady-state impedance during the applied sinusoidal voltage. Incandescent lighting is an example of such a load. The electrical motors not supplied through electronic converters also approximately meet this definition. The current or voltage waveforms will be almost sinusoidal, and their phase angles displaced depending on power factor of the electrical circuit. Transformers and rotating machines, under normal loading conditions, approximately meet this definition. Yet, it should be recognized that flux wave in the air gap of a rotating machine is not sinusoidal. Tooth ripples and slotting in rotating machines produce forward and reverse rotating harmonics. Magnetic circuits can saturate and generate harmonics. Saturation in a transformer on abnormally high voltage produces harmonics, as the relationship between magnetic flux density B and the magnetic field intensity H in a magnetic material (the transformer core) is not linear. Yet, the harmonics emissions from these sources are relatively small (Chapter 3).

In a nonlinear device, the application of a sinusoidal voltage does not result in a sinusoidal flow of current. These loads do not exhibit constant impedance during the entire cycle of applied sinusoidal voltage. *Nonlinearity is not the same as the frequency dependence of impedance*, that is, the reactance of a reactor changes in proportion to the applied frequency, but it is linear at each applied frequency if we neglect saturation and fringing. However, nonlinear loads draw a current that may even be discontinuous or flow in pulses for a part of the sinusoidal voltage cycle.

Mathematically, linearity implies two conditions:

- Homogeneity
- Superposition

Consider the state of a system defined in the state equation form:

$$\dot{x} = f[x(t), r(t), t] \tag{1.1}$$

If $x(t)$ is the solution to this differential equation with initial conditions $x(t_0)$ at $t = t_0$ and input $r(t)$, $t > t_0$:

$$x(t) = \varphi[x(t_0), r(t)] \tag{1.2}$$

then homogeneity implies that

$$\varphi[x(t_0), \alpha r(t)] = \alpha\varphi[x(t_0), r(t)] \tag{1.3}$$

where α is a scalar constant. This means that $x(t)$ with input $\alpha\, r(t)$ is equal to α times $x(t)$ with input $r(t)$ for any scalar α.

Superposition implies that

$$\varphi[x(t_0), r_1(t) + r_2(t)] = \varphi[x(t_0), r_1(t)] + \varphi[x(t_0), r_2(t)] \tag{1.4}$$

That is, $x(t)$ with inputs $r_1(t) + r_2(t)$ is equal to the sum of $x(t)$ with input $r_1(t)$ and $x(t)$ with input $r_2(t)$. Thus, linearity is superimposition plus homogeneity.

1.2 INCREASES IN NONLINEAR LOADS

Nonlinear loads are continuously on the increase. It is estimated that, during the next 10 years, more than 60% of the loads on utility systems will be nonlinear. Also much of the electronic load growth involves residential sector and household appliances. Concerns for harmonics originate from meeting a certain power quality, which leads to the related issues of (1) effects on the operation of electrical equipment, (2) harmonic analysis, and (3) harmonic control. A growing number of consumer loads are sensitive to poor power quality, and it is estimated that power quality problems cost US industry tens of billion of dollars per year. Although the expanded use of consumer automation equipment and power electronics is leading to higher productivity, these heavy loads are a source of electrical noise and harmonics and are less tolerant to poor power quality. For example, adjustable speed drives (ASDs) are less tolerant to voltage sags and swells as compared to an induction motor; and a voltage dip of 10% of certain time duration may precipitate ASD shutdown. These generate line harmonics and a source containing harmonics impacts their operation, leading to further generation of harmonics. *This implies that the nonlinear loads which are a source of generation of harmonics are themselves relatively less tolerant to the poor power quality that originates from harmonic emission from these loads.*

Some examples of nonlinear loads are as follows:

- ASD systems
- Cycloconverters
- Arc furnaces
- Rolling mills
- Switching mode power supplies
- Computers, copy machines, television sets, and home appliances
- Pulse burst modulation
- Static var compensators (SVCs)
- Thyristor-controlled reactors (TCRs)
- HVDC transmission, harmonics originate in converters
- Electric traction, chopper circuits
- Wind and solar power generation
- Battery charging and fuel cells
- Slip frequency recovery schemes of induction motors
- Fluorescent lighting and electronic ballasts
- Electrical vehicle charging systems
- Silicon-controlled rectifier (SCR) heating, induction heating, and arc welding.

The harmonics are also generated in conventional power equipment, such as transformer and motors. Saturation and switching of transformers generate harmonics. The harmonic generation is discussed in Chapters 3–5. The application of capacitor banks for power factor corrections and reactive power support can cause resonance and further distortions of waveforms (Chapter 9). Earlier rotating synchronous condensers have been replaced with modern shunt capacitors or SVCs (Chapter 4).

1.3 EFFECTS OF HARMONICS

Harmonics cause distortions of the voltage and current waveforms, which have adverse effects on electrical equipment. The estimation of harmonics from nonlinear loads is the first step in a harmonic analysis, and this may not be straightforward. There is an interaction between the harmonic producing equipment, which can have varied topologies, and the electrical system. Over the course of years, much attention has been focused on the analysis and control of harmonics, and standards have been established for permissible harmonic current and voltage distortions (Chapter 10). The effects of harmonics are discussed in Chapter 8.

1.4 DISTORTED WAVEFORMS

Harmonic emissions can have varied amplitudes and frequencies. The most common harmonics in power systems are sinusoidal components of a periodic waveform, which have frequencies that can be resolved into some multiples of the fundamental frequency. Fourier analysis is the mathematical tool employed for such analysis, and Chapter 2 provides an overview.

The components in a Fourier series that are not an integral multiple of the power frequency are called *noninteger harmonics* (Chapter 5).

The distortion produced by nonlinear loads can be resolved into a number of categories:

- A distorted waveform having a Fourier series with fundamental frequency equal to power system frequency and a periodic steady state exists. This is the most common case in harmonic studies. The waveform shown in Fig. 1.1 is synthesized from the harmonics shown in Table 1.1. The waveform in Fig. 1.1 is symmetrical about the x-axis and can be described by the equation:

$$I = \sin(\omega t - 30°) + 0.17\ \sin(5\omega t + 174°) + 0.12\ \sin(7\omega t + 101°) + \ \ldots$$

  Chapter 4 shows that this waveform is typically of a six-pulse current source converter, harmonics limited to 23rd, though higher harmonics will be present. The harmonic emission varies over wide range of distorted waveforms. Figure 1.2 shows a typical waveform for HVDC link, DC drives, and a six-pulse voltage source inverter (VSI) ASD, Ref. [1]. Chapter 4 studies typical waveforms and distortions from various types of power electronic

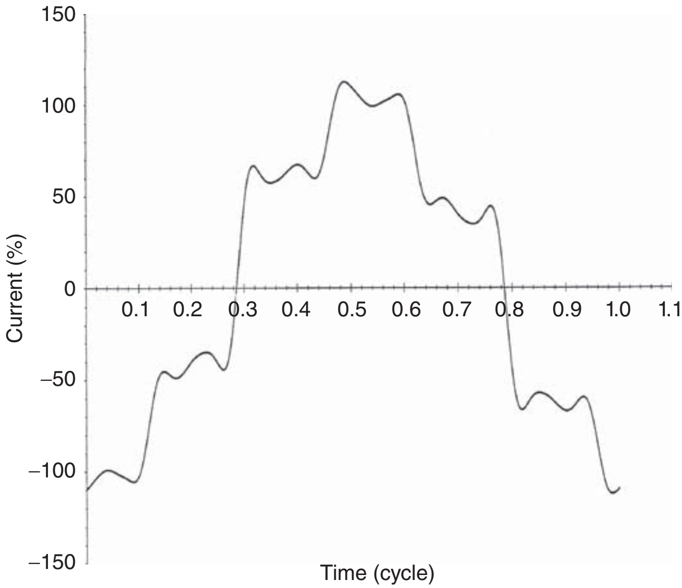

Figure 1.1 Simulated waveform of the harmonic spectrum shown in Table 1.1.

TABLE 1.1 Harmonic Content of the Waveform in Fig. 1.1

h	5	7	11	13	17	19	23
%	17	12	11	5	2.8	1.5	0.5

h = harmonic orders shown in percentage of fundamental current.

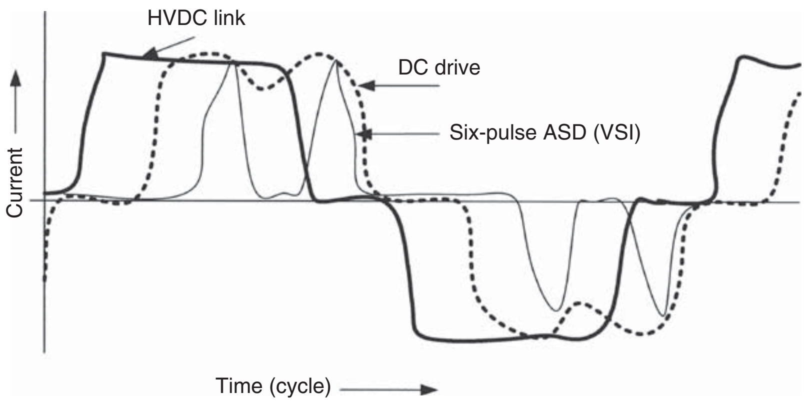

Figure 1.2 Typical line current waveforms of HVDC, DC drive, and six-pulse ASD.

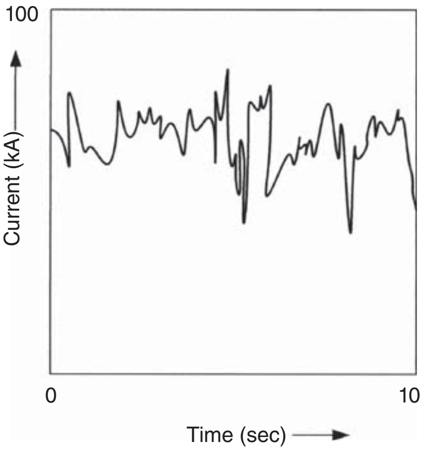

Figure 1.3 Erratic current signature of an electric arc furnace during scrap melting.

switching equipment. This is the most common situation in practice, and the distorted waveforms can be decomposed into a number of harmonics. The system can usually be modeled as a linear system.

- A distorted waveform having a submultiple of power system frequency and a periodic steady state exists. Certain types of pulsed loads and integral cycle controllers produce these types of waveforms (Chapters 4 and 5).
- The waveform is aperiodic, but perhaps almost periodic. A trigonometric series expansion may still exist. Examples are arcing devices: arc furnaces, fluorescent, mercury, and sodium vapor lighting. The process is not periodic in nature, and a periodic waveform is obtained if the conditions of operation are kept constant for a length of time. Consider the current signature of an arc furnace during scrap melting (Fig. 1.3). The waveform is highly distorted and aperiodic. Yet, typical harmonic emissions from arc furnace during melting and refining have been defined in IEEE standard 519 [5].

The arc furnace loads are highly polluting and cause phase unbalance, flicker, impact loading, harmonics, interharmonics, and resonance, and may give rise to torsional vibrations in rotating equipment.

1.4.1 Harmonics and Power Quality

Harmonics are one of the major power quality concerns. The power quality concerns embrace much wider concerns such as voltage sags and swells, transients, under and overvoltages, frequency variations, outright interruptions, power quality for sensitive electronic equipment such as computers. Table 3.1 summarizes some power quality problems. A reference of importance is IEEE Recommended Practice for Emergency and Standby Power Systems for Industrial and Commercial Applications, [6]. This book is not about power quality; however, some important publications are separately listed in References for the interested readers.

1.5 HARMONICS AND SEQUENCE COMPONENTS

The theory of sequence components is not discussed in this book and references [7–10] may be seen. In a three-phase balanced system under nonsinusoidal conditions, the hth-order harmonic voltage (or current) can be expressed as

$$V_{ah} = \sum_{h\neq 1} V_h(h\omega_0 t - \theta_h) \tag{1.5}$$

$$V_{bh} = \sum_{h\neq 1} V_h(h\omega_0 t - (h\pi/3)\theta_h) \tag{1.6}$$

$$V_{ch} = \sum_{h\neq 1} V_h(h\omega_0 t - (2h\pi/3)\theta_h) \tag{1.7}$$

Based on Eqs. (1.5–1.7) and counterclockwise rotation of the fundamental phasors, we can write

$$
\begin{aligned}
V_a &= V_1 \sin\omega t + V_2 \sin 2\omega t + V_3 \sin 3\omega t + V_4 \sin 4\omega t + V_5 \sin 5\omega t + \ldots. \\
V_b &= V_1 \sin(\omega t - 120^\circ) + V_2 \sin(2\omega t - 240^\circ) + V_3 \sin(3\omega t - 360^\circ) + V_4 \sin(4\omega t - 480^\circ) \\
&\quad + V_5 \sin(5\omega t - 600^\circ) + \ldots. \\
&= V_1 \sin(\omega t - 120^\circ) + V_2 \sin(2\omega t + 120^\circ) + V_3 \sin 3\omega t + V_4 \sin(4\omega t - 120^\circ) \\
&\quad + V_5 \sin(5\omega t + 120^\circ) + \ldots. \\
V_c &= V_1 \sin(\omega t + 120^\circ) + V_2 \sin(2\omega t + 240^\circ) + V_3 \sin(3\omega t + 360^\circ) + V_4 \sin(4\omega t + 480^\circ) \\
&\quad + V_5 \sin(5\omega t + 600^\circ) + \ldots. \\
&= V_1 \sin(\omega t + 120^\circ) + V_2 \sin(2\omega t - 120^\circ) + V_3 \sin 3\omega t + V_4 \sin(4\omega t + 120^\circ) \\
&\quad + V_5 \sin(5\omega t - 120^\circ) + \ldots.
\end{aligned}
$$

Under balanced conditions, the hth harmonic (frequency of harmonic = h times the fundamental frequency) of phase b lags h times 120° behind that of the same harmonic in phase a. The hth harmonic of phase c lags h times 240° behind that of the same harmonic in phase a. In the case of triplen harmonics, shifting the phase angles by three times 120° or three times 240° results in cophasial vectors.

Table 1.2 shows the sequence of harmonics, and the pattern is clearly positive–negative–zero. We can write

$$\text{Harmonics of the order } 3h+1 \text{ have positive sequence} \tag{1.8}$$

$$\text{Harmonics of the order } 3h+2 \text{ have negative sequence} \tag{1.9}$$

$$\text{Harmonics of the order } 3h \text{ are of zero sequence} \tag{1.10}$$

All triplen harmonics generated by nonlinear loads are zero sequence phasors. These add up in the neutral. In a three-phase four-wire system, with perfectly balanced

TABLE 1.2 Harmonic Order and Rotation

Harmonic Order	Forward	Reverse
Fundamental	x	
2		x
4	x	
5		x
7	x	
8		x
10	x	
11		x
13	x	
14		x
16	x	
17		x
19	x	
20		x
22	x	
23		x
25	x	
26		x
28	x	
29		x
31	x	

Note: The pattern is repeated for higher order harmonics.

single-phase loads between the phase and neutral, all positive and negative sequence harmonics will cancel out leaving only the zero sequence harmonics.

In an unbalanced three-phase system, serving single-phase load, the neutral carries zero sequence and the residual unbalance of positive and negative sequence currents. Even harmonics are absent in the line because of phase symmetry (Chapter 2), and unsymmetrical waveforms will add even harmonics to the phase conductors, for example, half-controlled three-phase bridge circuit discussed in Chapter 4.

1.5.1 Sequence Impedances of Power System Components

Positive, negative, and zero sequence impedances vary over large limits, depending on the power system equipment. For example, for transformers, positive and negative sequence impedances may be considered equal, but zero sequence impedance can be infinite depending on transformer winding connections and grounding. The zero sequence impedance of transmission lines can be two to three times that of the positive or negative sequence impedance. Even for fundamental frequency current flow, the accurate modeling of sequence impedances is important and the sequence impedances to harmonics must be modeled (Chapter 12).

1.6 HARMONIC INDICES

1.6.1 Harmonic Factor

An index of merit has been defined as a harmonic distortion factor [5] (harmonic factor). It is the ratio of the root mean square of the harmonic content to the root mean square value of the fundamental quantity, expressed as a percentage of the fundamental:

$$\mathrm{DF} = \sqrt{\frac{\sum \text{of squares of amplitudes of all harmonics}}{\text{Square of the amplitude of the fundamental}}} \times 100\% \tag{1.11}$$

The most commonly used index, total harmonic distortion (THD), which is in common use is the same as DF.

1.6.2 Equations for Common Harmonic Indices

We can write the following equations.

RMS voltage in presence of harmonics can be written as

$$V_{\mathrm{rms}} = \sqrt{\sum_{h=1}^{h=\infty} V_{h,\mathrm{rms}}^2} \tag{1.12}$$

And similarly, the expression for the current is

$$I_{\mathrm{rms}} = \sqrt{\sum_{h=1}^{h=\infty} I_{h,\mathrm{rms}}^2} \tag{1.13}$$

The total distortion factor for the voltage is

$$\mathrm{THD}_V = \frac{\sqrt{\sum_{h=2}^{h=\infty} V_{h,\mathrm{rms}}^2}}{V_{f,\mathrm{rms}}} \tag{1.14}$$

where $V_{f,\mathrm{rms}}$ is the fundamental frequency voltage. This can be written as

$$\mathrm{THD}_V = \sqrt{\left(\frac{V_{\mathrm{rms}}}{V_{f,\mathrm{rms}}}\right)^2 - 1} \tag{1.15}$$

or

$$V_{\mathrm{rms}} = V_{f,\mathrm{rms}}\sqrt{1 + \mathrm{THD}_V^2} \tag{1.16}$$

Similarly,

$$\mathrm{THD}_I = \frac{\sqrt{\sum_{h=2}^{h=\infty} I_{h,\mathrm{rms}}^2}}{I_{f,\mathrm{rms}}} = \sqrt{\left(\frac{I_{\mathrm{rms}}}{I_{f,\mathrm{rms}}}\right)^2 - 1} \tag{1.17}$$

$$I_{\mathrm{rms}} = I_{f,\mathrm{rms}}\sqrt{1 + \mathrm{THD}_I^2} \tag{1.18}$$

where $I_{f,\mathrm{rms}}$ is the fundamental frequency current.

The total demand distortion (TDD) is defined as

$$\mathrm{TDD} = \frac{\sqrt{\sum_{h=2}^{h=\infty} I_h^2}}{I_L} \tag{1.19}$$

where I_L is the load demand current.

The partial weighted harmonic distortion (PWHD) of current is defined as

$$\mathrm{PWHD}_I = \frac{\sqrt{\sum_{h=14}^{h=40} hI_h^2}}{I_{f,\mathrm{rms}}} \tag{1.20}$$

Similar expression is applicable for the voltage. The PWHD evaluates influence of current or voltage harmonics of higher order. The sum parameters are calculated with single harmonic current components I_h.

1.6.3 Telephone Influence Factor

Harmonics generate telephone Influence through inductive coupling. The telephone influence factor (TIF) for a voltage or current wave in an electrical supply circuit is the ratio of the square root of the sum of the squares of the weighted root mean square values of all the sine wave components (including AC waves both fundamental and harmonic) to the root mean square value (unweighted) of the entire wave:

$$\mathrm{TIF} = \frac{\sqrt{\sum W_f^2 I_f^2}}{I_{\mathrm{rms}}} \tag{1.21}$$

where I_f is the single frequency rms current at frequency f, W_f is the single frequency TIF weighting at frequency f. The voltage can be substituted for current. This definition may not be so explicit, see example in Chapter 8 for calculation. A similar expression can be written for voltage.

IT product is the inductive influence expressed in terms of the product of its root mean square magnitude I in amperes times its TIF.

$$\mathrm{IT} = \mathrm{TIF} * I_{\mathrm{rms}} = \sqrt{\sum (W_f I_f)^2} \tag{1.22}$$

kVT product is the inductive influence expressed in terms of the product of its root mean square magnitude in kV times its TIF.

$$\mathrm{kVT} = \mathrm{TIF} * \mathrm{kV}_{\mathrm{rms}} = \sqrt{\sum (W_f V_f)^2} \tag{1.23}$$

The telephone weighting factor that reflects the present C message weighting and the coupling normalized to 1 kHz is given by:

$$W_f = 5P_f f \tag{1.24}$$

where $P_f = C$ message weighting at frequency f under consideration. See Section 8.12 for further details.

1.7 POWER FACTOR, DISTORTION FACTOR, AND TOTAL POWER FACTOR

For sinusoidal voltages and currents, the power factor is defined as kW/kVA and the power factor angle ϕ is

$$\varphi = \cos^{-1}\frac{\mathrm{kW}}{\mathrm{kVA}} = \tan^{-1}\frac{\mathrm{kvar}}{\mathrm{kW}} \tag{1.25}$$

The power factor in presence of harmonics comprises two components: displacement and distortion. The effect of the two is combined in *total power factor*. The displacement component is the ratio of active power of the fundamental wave in watts to apparent power of fundamental wave in volt-amperes. This is the power factor as seen by the watt-hour and var-hour meters. The distortion component is the part that is associated with harmonic voltages and currents.

$$\mathrm{PF}_t = \mathrm{PF}_f \times \mathrm{PF}_{\mathrm{distortion}} \tag{1.26}$$

At fundamental frequency the displacement power factor will be equal to the total power factor, as the displacement power factor does not include kVA due to harmonics, while the total power factor does include it. For harmonic generating loads, the total power factor will always be less than the displacement power factor.

Continuing with the relation between power factor and displacement factor, the power factor of a converter with DC-link reactor is given by the expression from IEEE 519, Ref. [5]:

$$\text{Total PF} = \frac{q}{\pi}\sin\left(\frac{\pi}{q}\right) \tag{1.27}$$

where q is the number of converter pulses and π/q is the angle in radians (see Chapter 4). This ignores commutation overlap and no-phase overlap, and neglects transformer magnetizing current. For a six-pulse converter, the *maximum* power factor is $3/\pi = 0.955$. A 12-pulse converter has a theoretical *maximum* power factor of 0.988. The power factor drops drastically with the increase in firing angle.

Note that the power factor is a function of the drive topology, for example, with pulse width modulation, the input power factor is dependent on the type of converter only and the motor power factor is compensated by a capacitor in the DC link.

In the case of sinusoidal voltage and current, the following relationship holds

$$S^2 = P^2 + Q^2 \tag{1.28}$$

where P is the active power, Q is the reactive volt-ampere, and S is the volt-ampere. This relationship has been amply explored in load flow programs:

$$S = V_f I_f, \quad Q = V_f I_f \sin(\theta_f - \delta_f), \quad P = V_f I_f \cos(\theta_f - \delta_f), \quad \text{and} \quad \mathrm{PF} = P/S \tag{1.29}$$

$\theta_f - \delta_f =$ phase angle between fundamental voltage and fundamental current.

In the case of nonlinear load or when the source has nonsinusoidal waveform, the active power P can be defined as

$$P = \sum_{h=1}^{h=\infty} V_h I_h \cos(\theta_h - \delta_h) \tag{1.30}$$

Q can be written as

$$Q = \sum_{h=1}^{h=\infty} V_h I_h \sin(\theta_h - \delta_h) \tag{1.31}$$

V_h and I_h are in rms values, and the apparent power can be defined as

$$S = \sqrt{P^2 + Q^2 + D^2} \tag{1.32}$$

where D is the distortion power. Consider D^2 up to the third harmonic:

$$\begin{aligned} D^2 &= (V_0^2 + V_1^2 + V_2^2 + V_3^2)(I_0^2 + I_1^2 + I_2^2 + I_3^2) \\ &\quad - (V_0 I_0 + V_1 I_1 \cos\theta_1 + V_2 I_2 \cos\theta_2 + V_3 I_3 \cos\theta_3)^2 \\ &\quad - (V_1 I_1 \sin\theta_1 + V_2 I_2 \sin\theta_2 + V_3 I_3 \sin\theta_3)^2 \end{aligned} \tag{1.33}$$

An expression for distortion power factor can be arrived from current and voltage harmonic distortion factors. From the definition of these factors, rms harmonic voltages and currents can be written as

$$V_{\mathrm{rms}(h)} = V_f \sqrt{1 + \left(\frac{\mathrm{THD}_V}{100}\right)^2} \tag{1.34}$$

$$I_{\mathrm{rms}(h)} = I_f \sqrt{1 + \left(\frac{\mathrm{THD}_I}{100}\right)^2} \tag{1.35}$$

Therefore, the total power factor is

$$\mathrm{PF}_{\mathrm{tot}} = \frac{P}{V_f I_f \sqrt{1 + \left(\frac{\mathrm{THD}_V}{100}\right)^2} \sqrt{1 + \left(\frac{\mathrm{THD}_I}{100}\right)^2}} \tag{1.36}$$

Neglecting the power contributed by harmonics and also voltage distortion, as it is generally small, that is,

$$\mathrm{THD}_V \cong 0 \tag{1.37}$$

$$\begin{aligned}\mathrm{PF}_{\mathrm{tot}} &= \cos(\theta_f - \delta_f) \cdot \frac{1}{\sqrt{1 + \left(\frac{\mathrm{THD}_I}{100}\right)^2}} \\ &= \mathrm{PF}_{\mathrm{displacement}} \mathrm{PF}_{\mathrm{distortion}}\end{aligned} \tag{1.38}$$

The total power factor is the product of displacement power factor (which is the same as the fundamental power factor) and is multiplied by the distortion power factor as defined earlier.

The discussion is continued in Chapter 4. The modern trends in converter technology are to compensate for line harmonics and improve power factor to approximately unity simultaneously (Chapter 6).

1.8 POWER THEORIES

A number of power theories exist to explain the active, reactive, and instantaneous power relations in presence of harmonics, each fraught with some controversies:

1. Fryze theory in time domain
2. Shepherd and Zakikhani theory in frequency domain
3. Czarnecki power theory in frequency domain
4. Nabe and Akagi instantaneous power theory

See references [12–16].

1.8.1 Single-Phase Circuits: Sinusoidal

The instantaneous power is

$$p = vi = 2VI \sin \omega t \sin(\omega t - \theta) = p_a + p_q \tag{1.39}$$

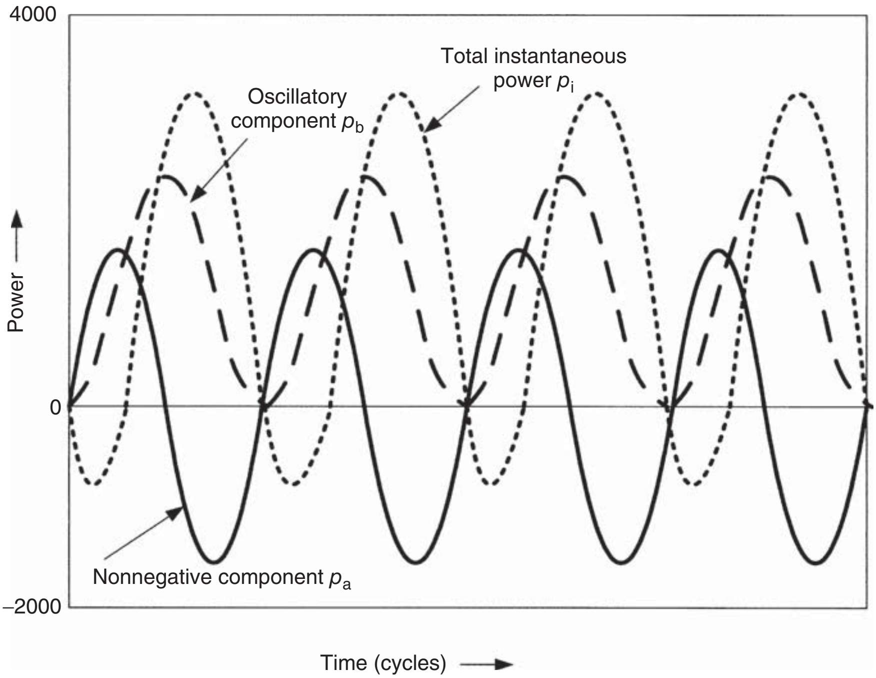

Figure 1.4 The waveform of separated components of instantaneous power in a single-phase circuit, with linear resistive-inductive load.

The active power also called real power is the average value of instantaneous power measured over a certain time period, say, τ to $\tau + kT$

We will denote instantaneous values in lowercase (v and i in (1.39) are in peak values).

$$p_a = VI\cos\theta[1 - \cos(2\omega t)] = P[1 - \cos(2\omega t]$$

$$p_q = -VI\sin\theta\ \sin(2\omega t) = -Q\ \sin(2\omega t) \tag{1.40}$$

The energy flows unidirectional from source to load $p_a \geq 0$. The instantaneous active power has two terms, active or real power and the intrinsic power $-P\ \cos 2\omega t$, which is always present when energy is transferred from source to load. If load is inductive $Q > 0$, and if load is capacitive $Q < 0$.

Figure 1.4 illustrates the instantaneous power components in single-phase circuits: the nonnegative component p_a, the oscillatory component p_b, and total instantaneous power p_i are shown.

1.8.2 Single-Phase Circuits: Nonsinusoidal

We can write

$$v = v_1 + v_H$$

$$i = i_1 + i_H$$

$$v_H = V_0 + \sqrt{2}\sum_{h\neq 1} V_h \sin(h\omega t - \alpha_h)$$

$$i_H = I_0 + \sqrt{2}\sum_{h\neq 1} I_h \sin(h\omega t - \beta_h) \tag{1.41}$$

v_1 and i_1 are power frequency components and v_H and i_H are other components.

The active power (rms value) is

$$p_a = V_0 I_0 + \sum_h V_h I_h \cos\theta_h[1 - \cos(2h\omega t - 2\alpha_h)] \tag{1.42}$$

It has two terms: $P_h = V_h I_h \cos\theta_h$ and the intrinsic harmonic power $-P_h \cos(2h\omega t - 2\alpha_h)$, which does not contribute to the net transfer of energy or additional power loss in the conductors.

Also, fundamental active power is

$$P_1 = V_1 I_1 \cos\theta_1 \tag{1.43}$$

And harmonic active power is

$$P_H = V_0 I_0 + \sum_{h\neq 1} V_h I_h \cos\theta_h = P - P_1 \tag{1.44}$$

P_q does not represent a net transfer of energy, its average value is nil. The current related to these nonactive components causes additional power loss in the conductors.

The apparent power is

$$S^2 = (V_1^2 + V_H^2)(I_1^2 + I_H^2) = S_1^2 + S_N^2 \tag{1.45}$$

where

$$\begin{aligned} S_N^2 &= (V_1 I_H)^2 + (V_H I_1)^2 + (V_H I_H)^2 \\ &= D_1^2 + D_V^2 + S_H^2 \end{aligned} \tag{1.46}$$

where

$$D_1 = \text{current distortion power (var)} = S_1(\text{THD}_I)$$

$$D_V = \text{voltage distortion power (var)} = S_1(\text{THD}_V)$$

$$S_H = \text{harmonic apparent power (VA)} = V_H I_H$$

$$= S_1(\text{THD}_I)(\text{THD}_V) = \sqrt{P_H^2 + D_H^2}$$

where D_H is the harmonic distortion power.

As THD_V is $\ll \mathrm{THD}_I$,

$$S_N = S_1(\mathrm{THD}_I)$$

The fundamental power factor is

$$\mathrm{PF}_1 = \cos\theta_1 = \frac{P_1}{S_1} \tag{1.47}$$

It is also called the displacement power factor.

And

$$\mathrm{PF} = P/S = \frac{[1 + (P_H/P_1)]\mathrm{PF}_1}{\sqrt{1 + \mathrm{THD}_I^2 + \mathrm{THD}_V^2 + (\mathrm{THD}_I\mathrm{THD}_V)^2}} \approx \frac{1}{\sqrt{1 + \mathrm{THD}_I^2}}\mathrm{PF}_1 \tag{1.48}$$

$$D_I > D_V > S_H > P_H$$

Equation (1.48) is the same as Eq. (1.38).

1.8.3 Three-Phase Systems

We can consider

- Balanced three-phase voltages and currents
- Asymmetrical voltages or load currents
- Nonlinear loads

Figure 1.5(a) shows balanced three-phase voltages and currents and balanced resistive load, and Fig. 1.5(b) depicts the instantaneous power in Fig. 1.5(a). The summation of phase instantaneous active powers in three phases is constant. Thus, the concepts arrived at in single-phase circuits cannot be applied. We examined that in single-phase circuits the active power has an intrinsic power component.

In three-phase circuits, it is impossible to separate reactive power on the basis of instantaneous power. Reactive power interpretation of single-phase circuits cannot be applied.

Figure 1.6 shows waveforms of voltages and currents in three-phase circuits with unbalanced resistive load. Now, the instantaneous active power is no longer constant. Considering three-phase circuit as three single-phase circuits leads to major misinterpretation of power phenomena.

Figure 1.7 depicts the symmetrical *nonlinear* load current and symmetrical waveforms of the supply voltage. Again the instantaneous active power is no longer constant. The individual instantaneous active powers in phases are shown in Fig. 1.8.

The extension of concept of apparent power in three-phase circuits has led to

Arithmetic apparent power:

$$V_aI_a + V_bI_b + V_cI_c = S_A \tag{1.49}$$

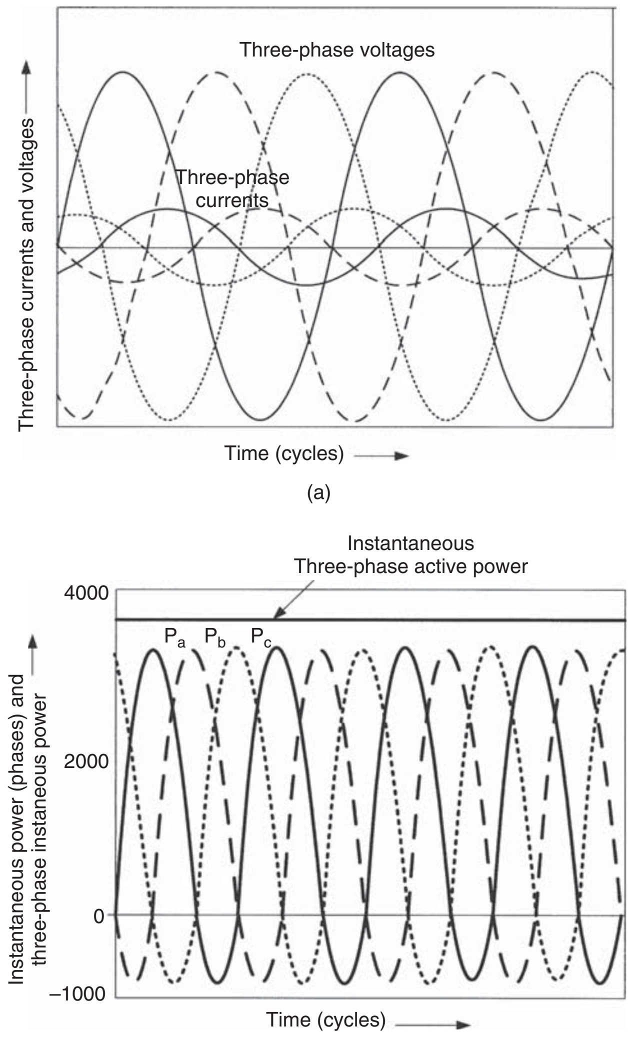

Figure 1.5 (a) Balanced three-phase voltages and currents in a three-phase system, (b) phase instantaneous powers, p_a, p_b, and p_c and total instantaneous power.

$V_a, V_b, \ldots\ I_a,\ \ I_b\ \ldots.$ in rms values.

Geometric apparent power:

$$S_G = \sqrt{P^2 + Q^2} \tag{1.50}$$

where three-phase active and reactive powers P and Q are

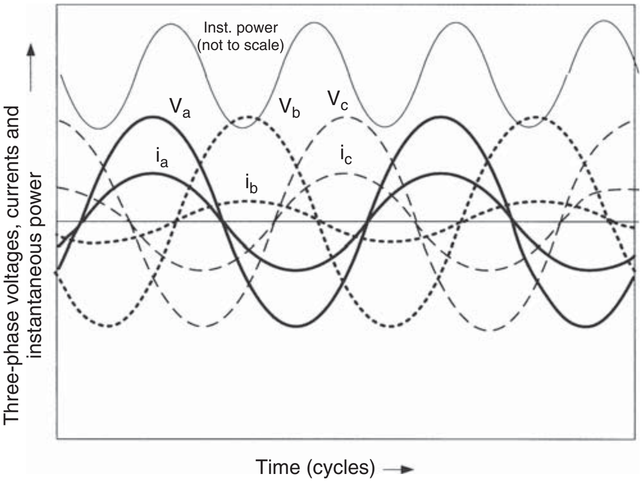

Figure 1.6 The waveform of the supply voltage and currents in a three-phase circuit with unbalanced resistive load and three-phase instantaneous active power.

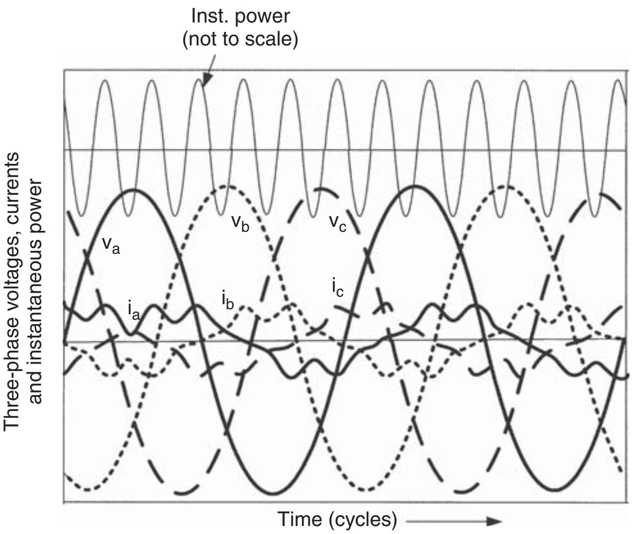

Figure 1.7 The waveforms of the supply voltage and current with *symmetrical* unbalanced load and three-phase instantaneous active power.

$$P = P_a + P_b + P_c$$
$$Q = Q_a + Q_b + Q_c \tag{1.51}$$

Buchholz apparent power:

$$S_B = \sqrt{V_a^2 + V_b^2 + V_c^2} \cdot \sqrt{I_a^2 + I_b^2 + I_c^2} \tag{1.52}$$

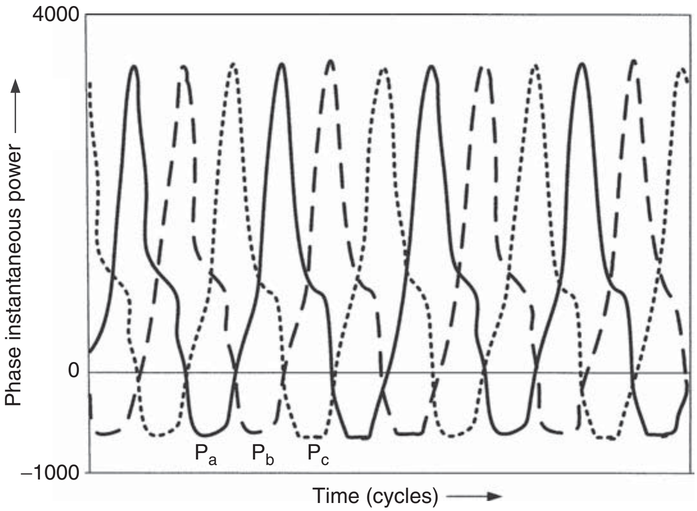

Figure 1.8 Phase instantaneous active powers for Fig. 1.7.

So long as the supply voltage is sinusoidal and symmetrical, and the load is balanced, these three relations (Eqs. (1.49), (1.51), and (1.52)) give the same correct result. If one of the above conditions is not met, the results will differ. Buchholz definition of apparent power allows correct calculation of apparent power.

We can define positive, negative, and zero sequence active and reactive powers:

$$P^{+} = 3V^{+}I^{+}\cos\theta^{+} \quad P^{-} = 3V^{-}I^{-}\cos\theta^{-} \quad P^{0} = 3V^{0}I^{0}\cos\theta^{0}$$

$$Q^{+} = 3V^{+}I^{+}\sin\theta^{+} \quad Q^{-} = 3V^{-}I^{-}\sin\theta^{-} \quad Q^{0} = 3V^{0}I^{0}\sin\theta^{0} \tag{1.53}$$

1.8.4 Nonsinusoidal and Unbalanced Three-Phase Systems

For nonsinusoidal and unbalanced three-phase systems, the following treatment can be applied:

Effective apparent power S_e can be written as

$$S_e^2 = p^2 + N^2 \tag{1.54}$$

where N is nonactive power and p is the active power.

In a three-phase three-wire system:

$$I_e = \sqrt{\frac{I_a^2 + I_b^2 + I_c^2}{3}}$$

$$I_{e1} = \sqrt{\frac{I_{a1}^2 + I_{b1}^2 + I_{c1}^2}{3}} = \text{fundamental}$$

$$I_{eH} = \sqrt{\frac{I_{aH}^2 + I_{bH}^2 + I_{cH}^2}{3}} = \sqrt{I_e^2 - I_{e1}^2} \tag{1.55}$$

Similar expressions can be written for voltages.

Resolution of S_e is implemented as

$$S_e^2 = S_{e1}^2 + S_{eN}^2 \tag{1.56}$$

S_{e1} is the fundamental apparent power and S_{eN} is nonfundamental apparent power.

$$S_{e1} = 3V_{e1}I_{e1}$$

$$S_{eN}^2 = D_{e1}^2 + D_{ev}^2 + S_{eH}^2 = 3V_{e1}I_{eH} + 3V_{eH}I_{e1} + 3V_{eH}I_{eH} \tag{1.57}$$

$$S_{eN} = \sqrt{\text{THD}_{eI}^2 + \text{THD}_{eV}^2 + (\text{THD}_{eI}\text{THD}_{eV})^2} \tag{1.58}$$

where

$$D_{eI} = S_{e1}(\text{THD}_{eI}) \quad D_{eV} = S_{e1}(\text{THD}_{eV}) \quad D_{eH} = S_{e1}(\text{THD}_{eV})(\text{THD}_{eI}) \tag{1.59}$$

are the components of nonfundamental apparent power.

The load unbalance can be evaluated using unbalance power:

$$S_{U1} = \sqrt{S_{e1}^2 - (S_1^+)^2} \tag{1.60}$$

where

$$S_1^+ = \sqrt{(P_1^+)^2 + (Q_1^+)^2} \tag{1.61}$$

Here,

$$P_1^+ = 3V_1^+I_1^+ \cos\theta_1^+$$

$$Q_1^+ = 3V_1^+I_1^+ \sin\theta_1^+$$

The fundamental positive sequence power factor is

$$PF_1^+ = \frac{P_1^+}{S_1^+} \tag{1.62}$$

It plays the same role as the fundamental power factor has in nonsinusoidal single-phase circuits.

The combined power factor is

$$PF = \frac{P}{S_e} \tag{1.63}$$

Table 1.3 shows these relations.

TABLE 1.3 Three-Phase Systems with Nonsinusoidal Waveforms

Quantity or Indicator	Combined	Fundamental Powers	Nonfundamental Powers
Apparent	S_e (VA)	S_{e1} S_1^+ S_{U1} (VA)	S_{eN} S_{eH} (VA)
Active	P (W)	P_1^+ (W)	P_H (W)
Nonactive	N (var)	Q_1^+ (var)	D_{eI} D_{eV} D_{eH} (var)
PF	P/S_e	P_1^+/S_1^+	
Harmonic pollution			S_{eN}/S_{e1}
Load unbalance		S_{U1}/S_1^+	

Source: Ref. [11].

Example 1.1: This example is based on Ref. [13]. Consider nonsinusoidal voltage and currents containing harmonics of the order of 3rd, 5th, and 7th.

$$v = v_1 + v_3 + v_5 + v_7 = \sqrt{2} \sum_{h=1,3,5,7} V_h \sin(h\omega t - \alpha_h)$$

$$i = i_1 + i_3 + i_5 + i_7 = \sqrt{2} \sum_{h=1,3,5,7} I_h \sin(h\omega t - \beta_h)$$

Then,

$$p = p_{hh} + p_{mn}$$

$$p_{hh} = v_1 i_1 + v_3 i_3 + v_5 i_5 + v_7 i_7$$

$$p_{mn} = v_1(i_3 + i_5 + i_7) + v_3(i_1 + i_5 + i_7) + v_5(i_1 + i_3 + i_7) + v_7(i_1 + i_3 + i_5)$$

P_{mn} is the instantaneous power that contains only cross terms.

The direct product yields

$$\begin{aligned} v_h i_h &= \sqrt{2} V_h \sin(h\omega t - \alpha_h) \sqrt{2} I_h \sin(h\omega t - \beta_h) \\ &= P_h[1 - \cos(2h\omega t - 2\alpha_h)] - Q_h \sin(2h\omega t - 2\alpha_h) \end{aligned}$$

where

$$P_h = V_h I_h \cos(\theta_h) \quad Q_h = V_h I_h \sin(\theta_h)$$

are the harmonic active and reactive powers of order h, and $\theta_h = (\beta_h - \alpha_h)$ is the phase angle between phasors V_h and I_h.

The total active power is

$$P = \sum_{h=1,3,5,7} P_h = P_1 + P_H$$

where

$$P_1 = V_1 I_1 \cos\theta_1 \quad P_H = P_3 + P_5 + P_7$$

For *each* harmonic

$$S_h = \sqrt{P_h^2 + Q_h^2}$$

The total apparent power squared is

$$\begin{aligned}S^2 &= V^2I^2 = (V_1^2 + V_3^2 + V_5^2 + V_7^2)(I_1^2 + I_3^2 + I_5^2 + I_7^2)\\ &= V_1^2I_1^2 + V_3^2I_3^2 + V_5^2I_5^2 + V_7^2I_7^2 + V_1^2(I_3^2 + I_5^2 + I_7^2) + I_1^2(V_3^2 + V_5^2 + V_7^2)\\ &\quad + V_3^2I_5^2 + V_3^2I_7^2 + V_5^2I_3^2 + V_5^2I_7^2 + V_7^2I_3^2 + V_7^2I_5^2\end{aligned}$$

or

$$\begin{aligned}S^2 &= S_1^2 + S_3^2 + S_5^2 + S_7^2 + D_I^2 + D_V^2 + D_{35}^2 + D_{37}^2 + D_{53}^2 + D_{57}^2 + D_{73}^2 + D_{75}^2\\ &= S_1^2 + S_N^2\end{aligned}$$

where

$$S_1^2 = P_1^2 + Q_1^2$$

$$S_N^2 = D_I^2 + D_V^2 + S_H^2$$

If the load is supplied by a line having a resistance r, the power loss in the line is

$$\Delta P = \frac{r}{V^2}(P_1^2 + Q_1^2 + D_I^2 + D_V^2 + S_H^2) = \frac{r}{V^2}(S_1^2 + S_N^2)$$

Note that distortion power and harmonic power contribute to the losses.

Consider following instantaneous currents and voltages:

$$v_1 = \sqrt{2}\cdot 100\ \sin(\omega t - 0°) \quad i_1 = \sqrt{2}\cdot 100\ \sin(\omega t - 30°)$$

$$v_3 = \sqrt{2}\cdot 8\ \sin(3\omega t - 70°) \quad i_3 = \sqrt{2}\cdot 20\ \sin(3\omega t - 165°)$$

$$v_5 = \sqrt{2}\cdot 15\ \sin(5\omega t + 140°) \quad i_5 = \sqrt{2}\cdot 15\ \sin(5\omega t + 234°)$$

$$v_7 = \sqrt{2}\cdot 5\ \sin(7\omega t + 20°) \quad i_7 = \sqrt{2}\cdot 10\ \sin(7\omega t + 234°)$$

The calculated active powers are shown in Table 1.4. The total harmonic power $P_H = -27.46 < 0°$ is supplied by the load and injected into the power system. This is typical for dominant nonlinear loads. Bulk of the power is supplied to the load by fundamental component.

The reactive powers are shown in Table 1.5. Q_5 is negative, while all others are positive. Note that it will be incorrect to arithmetically add the reactive powers, and it will give incorrect power loss due to reactive power. The arithmetic sum of reactive powers is 4984.67 var. Then the reactive power loss calculated in a resistance of 1 ohm and voltage of 240 volts is

TABLE 1.4 Active Powers, Example 1.1

P_1 (W)	P_3 (W)	P_5 (W)	P_7 (W)	P (W)	P_H (W)
8660.00	−13.94	−11.78	−1.74	8632.54	−27.46

Source: Ref. [11].

TABLE 1.5 Reactive Powers, Example 1.1

Q_1 (var)	Q_3 (var)	Q_5 (var)	Q_7 (var)
5000.00	159.39	−224.69	49.97

Source: Ref. [11].

TABLE 1.6 Distortion Powers and Their Components, Example 1.1

D_{13} (var)	D_{15} (var)	D_{17} (var)	D_I (var)
2000.00	1500.00	1000.00	2692.58
D_{31} (var)	D_{51} (var)	D_{71} (var)	D_V (var)
800.00	1500.00	500.00	1772.00

Source: Ref. [11].

$$\Delta P_B = \frac{r}{V^2}(4984.67)^2 = 431.37\,\mathrm{W}$$

This is incorrect. It should be calculated as

$$\Delta P = \frac{r}{V^2}(Q_1^2 + Q_3^2 + Q_5^2 + Q_7^2) = 435.39\,\mathrm{W}$$

The cross products that produce distortion powers are in Table 1.6, and the cross products that belong to *harmonic* apparent power are in Table 1.7.

The system has $V = 101.56$ V, $I = 103.56$A, $\mathrm{THD}_V = 0.177$, $\mathrm{THD}_I = 0.269$, fundamental power factor $\mathrm{PF}_1 = 0.866$, $\mathrm{PF} = 0.821$.

The power components are shown in Fig. 1.9.

1.8.5 Instantaneous Power Theory

The Nabe–Akagi instantaneous reactive power p–q theory is based on Clark's component transformations [10] and provides power properties in three-phase circuits. Figure 1.10 shows the transformation of $a - b - c$ coordinates into $\alpha - \beta - 0$ coordinates. The description of power properties of the electrical circuits using instantaneous voltage and current values without the use of Fourier series generates interest in this theory, used for switching compensators and active filter controls.

The instantaneous power method calculates the desired current so that the instantaneous active power and reactive power in a three-phase system are kept constant, that is, the active filter compensates for variation in instantaneous power [17].

By linear transformation, the phase voltages e_a, e_b, e_c and load currents i_a, i_b, i_c are transformed into an $\alpha - \beta$ (two-phase) coordinate system:

$$\begin{vmatrix} e_\alpha \\ e_\beta \end{vmatrix} = \sqrt{\frac{2}{3}} \begin{vmatrix} 1 & -\frac{1}{2} & -\frac{1}{2} \\ 0 & \frac{\sqrt{3}}{2} & -\frac{\sqrt{3}}{2} \end{vmatrix} \begin{vmatrix} e_a \\ e_b \\ e_c \end{vmatrix} \tag{1.64}$$

and

$$\begin{vmatrix} i_\alpha \\ i_\beta \end{vmatrix} = \sqrt{\frac{2}{3}} \begin{vmatrix} 1 & -\frac{1}{2} & -\frac{1}{2} \\ 0 & \frac{\sqrt{3}}{2} & -\frac{\sqrt{3}}{2} \end{vmatrix} \begin{vmatrix} i_a \\ i_b \\ i_c \end{vmatrix} \tag{1.65}$$

The instantaneous real power ρ and the instantaneous imaginary power q are defined as

$$\begin{vmatrix} p \\ q \end{vmatrix} = \begin{vmatrix} e_\alpha & e_\beta \\ -e_\beta & e_\alpha \end{vmatrix} \begin{vmatrix} i_\alpha \\ i_\beta \end{vmatrix} \tag{1.66}$$

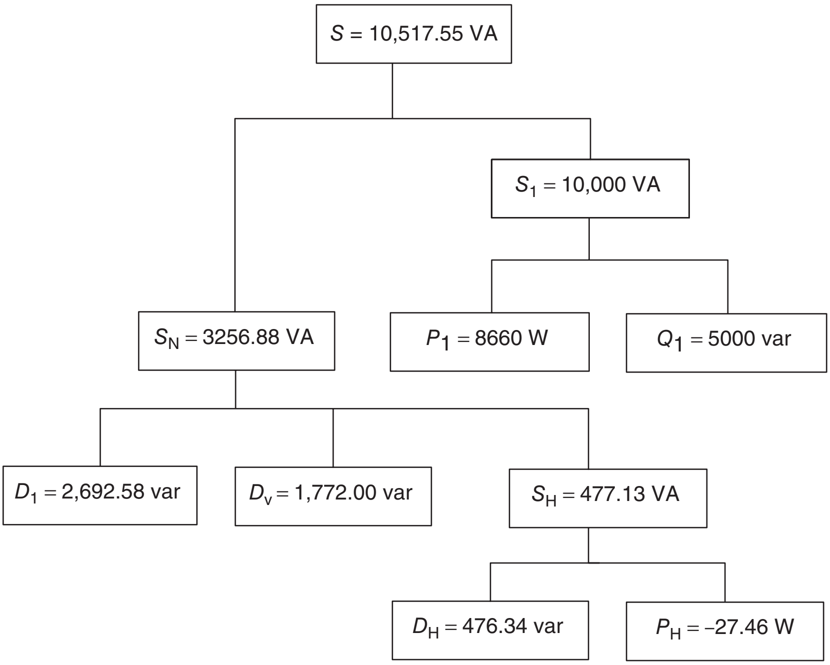

Figure 1.9 Calculations tree of various power components, Example 1.1.

TABLE 1.7 Distortion Harmonic Powers, Example 1.1

D_{35} (var)	D_{37} (var)	D_{53} (var)	D_{57} (var)	D_{73} (var)	D_{75} (var)
120.00	80.00	300.00	150.00	100.00	75.00

Source: Ref. [11].

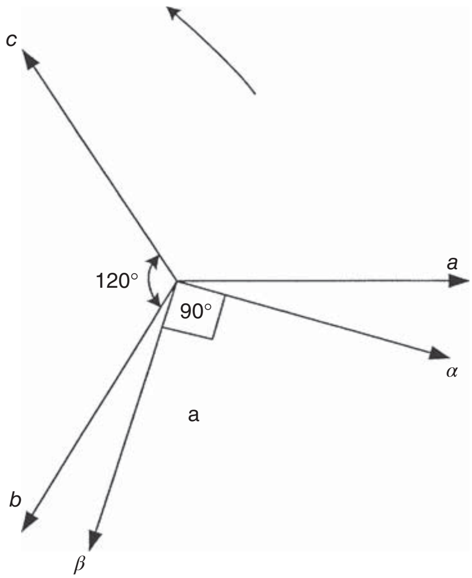

Figure 1.10 Transformation of $a-b-c$ coordinates into $\alpha-\beta-0$ coordinates, $p-q$ theory.

Here, p and q are not conventional watts and vars. The p and q are defined by the instantaneous voltage in one phase and the instantaneous current in the other phase:

$$p = e_\alpha i_\alpha + e_\beta i_\beta = e_a i_a + e_b i_b + e_c i_c \tag{1.67}$$

To define instantaneous reactive power, the space vector of imaginary power is defined as

$$\begin{aligned} q &= e_\alpha i_\beta + e_\beta i_\alpha \\ &= \frac{1}{\sqrt{3}}[i_a(e_c - e_b) + i_b(e_a - e_c) + i_c(e_b - e_a)] \end{aligned} \tag{1.68}$$

Equation (1.66) can be written as

$$\begin{vmatrix} i_\alpha \\ i_\beta \end{vmatrix} = \begin{vmatrix} e_\alpha & e_\beta \\ -e_\beta & e_\alpha \end{vmatrix}^{-1} \begin{vmatrix} p \\ q \end{vmatrix} \tag{1.69}$$

These are divided into two kinds of currents:

$$\begin{vmatrix} i_\alpha \\ i_\beta \end{vmatrix} = \begin{vmatrix} e_\alpha & e_\beta \\ -e_\beta & e_\alpha \end{vmatrix}^{-1} \begin{vmatrix} p \\ 0 \end{vmatrix} + \begin{vmatrix} e_\alpha & e_\beta \\ -e_\beta & e_\alpha \end{vmatrix}^{-1} \begin{vmatrix} 0 \\ q \end{vmatrix} \tag{1.70}$$

This can be written as

$$\begin{vmatrix} i_\alpha \\ i_\beta \end{vmatrix} = \begin{vmatrix} i_{\alpha p} \\ i_{\beta p} \end{vmatrix} + \begin{vmatrix} i_{\alpha q} \\ i_{\beta q} \end{vmatrix} \tag{1.71}$$

where $i_{\alpha p}$ is the α-axis instantaneous active current:

$$i_{\alpha p} = \frac{e_\alpha}{e_\alpha^2 + e_\beta^2} p \tag{1.72}$$

$i_{\alpha q}$ is the α-axis instantaneous reactive current:

$$i_{\alpha q} = \frac{-e_\beta}{e_\alpha^2 + e_\beta^2} q \tag{1.73}$$

$i_{\beta p}$ is the β-axis instantaneous active current:

$$i_{\beta p} = \frac{e_\alpha}{e_\alpha^2 + e_\beta^2} p \tag{1.74}$$

and $i_{\beta q}$ is the β-axis instantaneous reactive current:

$$i_{\beta q} = \frac{e_\alpha}{e_\alpha^2 + e_\beta^2} q \tag{1.75}$$

The following equations exist:

$$\begin{aligned} p &= e_\alpha i_{\alpha P} + e_\beta i_{\beta P} \equiv P_{\alpha P} + P_{\beta P} \\ 0 &= e_\alpha i_{\alpha q} + e_\beta i_{\beta q} \equiv P_{\alpha q} + P_{\beta q} \end{aligned} \tag{1.76}$$

where the α-axis instantaneous active and reactive powers are

$$P_{\alpha p} = \frac{e_\alpha^2}{e_\alpha^2 + e_\beta^2} p \quad P_{\alpha q} = \frac{-e_\alpha e_\beta}{e_\alpha^2 + e_\beta^2} q \tag{1.77}$$

The β-axis instantaneous active power and reactive power are

$$P_{\beta q} = \frac{e_\beta^2}{e_\alpha^2 + e_\beta^2} p \quad P_{\beta q} = \frac{e_\alpha e_\beta}{e_\alpha^2 + e_\beta^2} q \tag{1.78}$$

The sum of the instantaneous active powers in two axes coincides with the instantaneous real power in the three-phase circuit. The instantaneous reactive powers P_{aq} and $P_{\beta q}$ cancel each other and make no contribution to the instantaneous power flow from the source to the load.

Consider instantaneous power flow in a three-phase cycloconverter. The instantaneous reactive power on the source side is the instantaneous reactive power circulating between source and cycloconverter while the instantaneous reactive power on the output side is the instantaneous reactive power between the cycloconverter and the load. Therefore, there is no relationship between the instantaneous reactive powers on the input and output sides, and the instantaneous imaginary power on the input side is not equal to the instantaneous imaginary power on the output side. However, assuming zero active power loss in the converter, the instantaneous real power on the input side is equal to the real output power. An application to active filters is discussed in Chapter 6.

The author in Ref. [15] critiques this theory that it suggests an erroneous interpretation of three-phase power circuits. According to the theory, instantaneous imaginary current can occur in the current of a load with zero reactive power, Also instantaneous active current may occur in the current of a load with zero active power.

1.9 AMPLIFICATION AND ATTENUATION OF HARMONICS

Harmonics originating from their source are propagated in the power systems and their impact can be present at a distance [18]. In this process, the harmonics can be either amplified or mitigated. Capacitor banks in the power system are a major source of harmonic amplifications and waveform distortions. Many different types of harmonic sources may be dispersed throughout the system, and the current and voltage distortions due to these become of concern. Utilities must maintain a certain voltage quality at the consumer premises and, in turn, the harmonics injected into the power systems by a consumer must be controlled and limited. The nature of power system: industrial plant distributions, commercial distribution systems, and utility distribution or transmission systems are important in this aspect. An analysis requires correct estimation of the harmonic generation at a certain point in the power systems, modeling of system components and harmonics themselves for accurate results, for example, constant current injection models for all types of harmonic generation may not be accurate. Based on the accurate harmonic analysis, provisions of active harmonic mitigation strategies at the source of harmonic generation can be applied to limit the harmonics. Passive filters are another important option, especially in large Mvar ratings. These subjects are covered in this book.

New Power Conversion Techniques

Advances in power electronics have resulted in techniques for improving the current wave shape and power factor simultaneously, minimizing the filter requirements [19]. In general, these systems use high-frequency switching to achieve greater flexibility in power conversion and can reduce the lower order harmonics also. Distortion is created at high-frequency switching, which is generally above 20 kHz, and the distortion cannot penetrate into the system (see Chapter 6).

Some publications (books only) on harmonics are separately listed in References. Also some important ANSI/IEEE standards, though referenced appropriately in the rest of the book, are listed.

REFERENCES

1. IEEE Working Group on Power System Harmonics. "Power system harmonics: an overview," IEEE Transactions on Power Apparatus and Systems PAS, vol. 102, pp. 2455–2459, 1983.
2. E. L. Owen, "A history of harmonics in power systems," IEEE Industry Application Magazine, vol. 4, no. 1, pp. 6–12, 1998.
3. M. E. Baran and N. R. Mahajan, "DC distribution for industrial systems: opportunities and challenges," IEEE Transactions on Industry Applications, vol. 39, no. 6, pp. 1596–1601, 2003.
4. J. G. Ciezki and R. W. Ashton, "Selection and stability issues associated with a navy shipboard DC zonal electrical distribution system," IEEE Transactions on Power Delivery, vol. 15, pp. 665–669, 2000.
5. IEEE Standard 519, IEEE recommended practices and requirements for harmonic control in power systems, 1992.
6. ANSI/IEEE Standard 446, IEEE recommended practice for emergency and standby power systems for industrial and commercial applications, 1987.
7. G. O. Calabrase. Symmetrical Components Applied to Electrical Power Networks, Ronald Press Group, New York, 1959.
8. J. L. Blackburn. Symmetrical Components for Power Systems Engineering, Marcel Dekker, New York, 1993.
9. Westinghouse. Westinghouse Transmission and Distribution Handbook, Fourth Edition, Pittsburgh, 1964.
10. J. C. Das. Power System Analysis, Short Circuit Load Flow and Harmonics, 2nd Edition, CRC Press, 2012.
11. L. S. Czarnecki. "What is wrong with Budenu's concept of reactive power and distortion power and why it should be abandoned," IEEE Transactions on Instrumentation and Measurement, vol. IM-36, no. 3, 1987.
12. IEEE Working Group on Non-Sinusoidal Situations. "Practical definitions for powers in systems with non-sinusoidal waveforms and unbalanced loads," IEEE Transactions on Power Delivery, vol. 11, no. 1, pp. 79–101, 1996.
13. IEEE Std. 1459. IEEE standard definitions for the measurement of electrical power quantities under sinusoidal, nonsinusoidal, balanced or unbalanced conditions, 2010.
14. N. L. Kusters and W. J. M. Moore. "On the definition of reactive power under nonsinusoidal conditions," IEEE Transactions on Power Applications, vol. PAS-99, pp. 1845–1854, 1980.
15. L. S. Czarnecki. Energy Flow and Power Phenomena in Electrical Circuits: Illusions and Reality. Springer Verlag, Electrical Engineering, 2000.
16. S. W. Zakikhani. "Suggested definition of reactive power for nonsinusoidal systems," IEE Proceedings, no. 119, pp. 1361–1362, 1972.
17. H. Akagi and A. Nabe. "The p-q theory in three-phase systems under non-sinusoidal conditions," ETEP, vol. 3, pp. 27–30, 1993.
18. A. E. Emanual. "On the assessment of harmonic pollution," IEEE Transactions on Power Delivery, vol. 10, no. 3, pp. 1693–1698, 1995.
19. F. L. Luo and H. Ye. Power Electronics, CRC Press, Boca Raton, FL, 2010.

Books on Power System Harmonics

20. E. Acha and M. Madrigal. Power System Harmonics: Computer Modeling and Analysis, John Wiley & Sons, 2001
21. J. Arrillaga, B. C. Smith, N. R. Watson and A. R. Wood. Power System Harmonic Analysis, John Wiley & Sons, 2000
22. J. Arrillaga and N. R. Watson. Power System Harmonics, 2nd Edition, John Wiley & Sons, 2003.
23. F. C. De La Rosa, Harmonics and Power Systems, CRC Press, 2006.
24. G. J. Wakileh. Power System Harmonics: Fundamentals, Analysis and Filter Design, Springer, 2001.
25. J. C. Das. Power System Analysis, Short Circuit Load Flow and Harmonics, 2nd Edition, CRC Press, 2012.

26. S. M. Ismail, S. F. Mekhamer and A. Y. Abdelaziz. Power System Harmonics in Industrial Electrical Systems-Techno-Economical Assessment, Lambert Academic Publishing, 2013.
27. A. Fadnis, Harmonics in Power Systems: Effects of Power Switching Devices in Power Systems, Lambert Academic Publishing, 2012.
28. A. Nassif, Harmonics in Power Systems-Modeling, Measurement and Mitigation, CRC Press, 2010.
29. E.W. Kimbark. Direct Current Transmission, Vol. 1, John Wiley & Sons, New York, 1971.

Books on Power Quality

30. J. Arrillaga, S. Chen and N. R. Watson, Power Quality Assessment, John Wiley & Sons, 2000.
31. A. Baggini, Handbook of Power Quality, John Wiley & Sons, 2008
32. M. H. J. Bollen, Understanding Power Quality Problems, IEEE, 2000.
33. B. Kennedy, Power Quality Primer, McGraw-Hill, 2000.
34. R. C. Dugan, M. F. McGranaghan and H. W. Beaty, Electrical Power Systems Quality, McGraw-Hill, 1976.
35. E.F. Fuchs and M.A.S. Masoum, Power Quality in Power Systems and Electrical Machines, Elsevier, 2008.
36. A. Ghosh and G. Ledwich, Power Quality Enhancement Using Custom Power Devices, Kulwar Academic Publishers, Norwell, MA, 2002.
37. G. T. Heydt, Electrical Power Quality, 2nd Edition, Stars in a Circle Publications, 1991.
38. A. Kusko, and M. T. Thompson, Power Quality in Electrical Systems, McGraw-Hill Professional, 2007.
39. W. Mielczarski, G. J. Anders, M. F. Conlon, W. B. Lawrence, H. Khalsa, and G. Michalik, Quality of Electricity Supply and Management of Network Losses, Puma Press, Melbourne, 1997.
40. A. Moreno-Muoz (Ed.) Power Quality Mitigation Technologies in a Distributed Environment, Springer, 2007.
41. C. Sankran, Power Quality, CRC Press, 2002.

Major IEEE Standards Related to Harmonics

42. IEEE Standard 519, IEEE recommended practices and requirements for harmonic control in power systems, 1992.
43. IEEE Standard C37.99, IEEE Guide for Protection of Shunt Capacitor Banks, 2000
44. IEEE P519.1/D9a. Draft for applying harmonic limits on power systems, 2004.
45. ANSI/IEEE Standard C37.99, Guide for protection of shunt capacitor banks, 2000.
46. IEEE P1036/D13a. Draft Guide for Application of Shunt Power Capacitors, 2006.
47. IEEE Standard C57.110. IEEE recommended practice for establishing liquid-filled and dry-type power and distribution transformer capability when supplying nonsinusoidal load currents, 2008.
48. IEEE Standard 18. IEEE standard for shunt power capacitors, 2002.
49. IEEE Standard 1531, IEEE guide for application and specifications of harmonic filters, 2003.

CHAPTER 2

FOURIER ANALYSIS

The French mathematician J. B. J. Fourier (1758–1830) showed that arbitrary periodic functions could be represented by an infinite series of sinusoids of harmonically related frequencies. This was related to heat flow as the electrical applications were not developed at that time. We first define periodic functions.

2.1 PERIODIC FUNCTIONS

A function is said to be periodic if it is defined for all real values of t and if there is a positive number T such that

$$f(t) = f(t+T) = f(t+2T) = f(t+nT) \tag{2.1}$$

then T is called the period of the function.

If k is any integer and $f(t+kT) = f(t)$ for all values of t and if two functions $f_1(t)$ and $f_2(t)$ have the same period T, then the function $f_3(t) = af_1(t) + bf_2(t)$, where a and b are constants, also has the same period T. Figure 2.1 shows periodic functions.

The functions

$$f_1(t) = \cos\frac{2\pi n}{T}t = \cos n\omega_0 t$$

$$f_2(t) = \sin\frac{2\pi n}{T}t = \sin n\omega_0 t \tag{2.2}$$

are of special interest. Each frequency of the sinusoids $n\omega_0$ is said to be of nth harmonic of the fundamental frequency ω_0, and each of these frequencies is related to period t.

2.2 ORTHOGONAL FUNCTIONS

Two functions $f_1(t)$ and $f_2(t)$ are orthogonal over the interval (T_1, T_2) if

$$\int_{T_1}^{T_2} f_1(t) f_2(t) = 0 \tag{2.3}$$

Power System Harmonics and Passive Filter Designs, First Edition. J.C. Das.

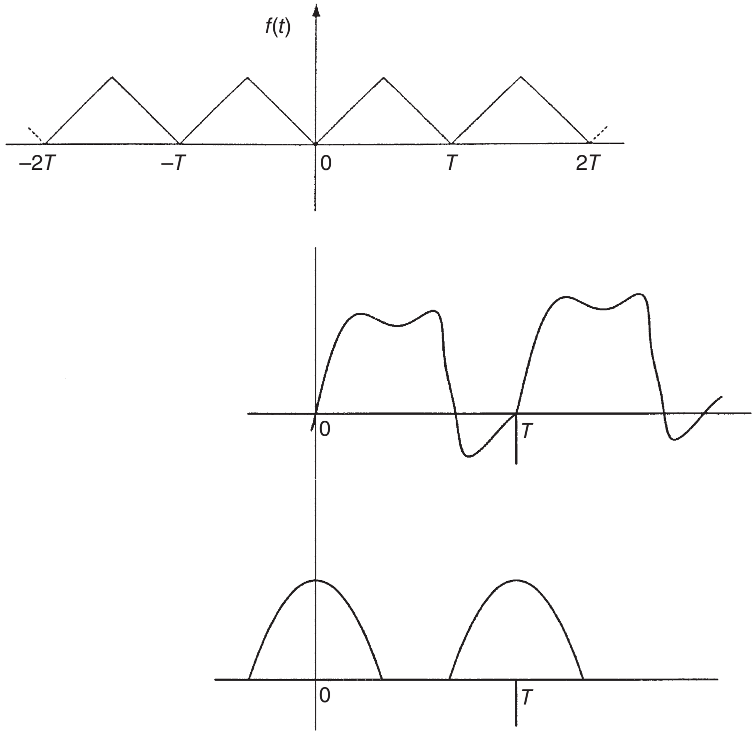

Figure 2.1 Periodic functions.

Figure 2.2 shows the orthogonal functions over a period T. Observe that

$$\int_0^T \sin \ m\omega_0 t \ \ dt = 0 \quad \text{all} \ \ m$$

$$\int_0^T \cos \ n\omega_0 t \ \ dt = 0 \quad \text{all} \ \ n \neq 0 \tag{2.4}$$

The average value of a sinusoid over m or n complete cycles is zero; therefore, the following three cross products are also zero.

$$\int_0^T \sin m\omega_0 t \, dt . \cos n\omega_0 t \, dt = 0 \quad \text{all} \ \ m, n$$

$$\int_0^T \sin m\omega_0 t \, dt . \sin n\omega_0 t \, dt = 0 \quad m \neq n$$

$$\int_0^T \cos m\omega_0 t \, dt . \cos n\omega_0 t \, dt = 0 \quad m \neq n \tag{2.5}$$

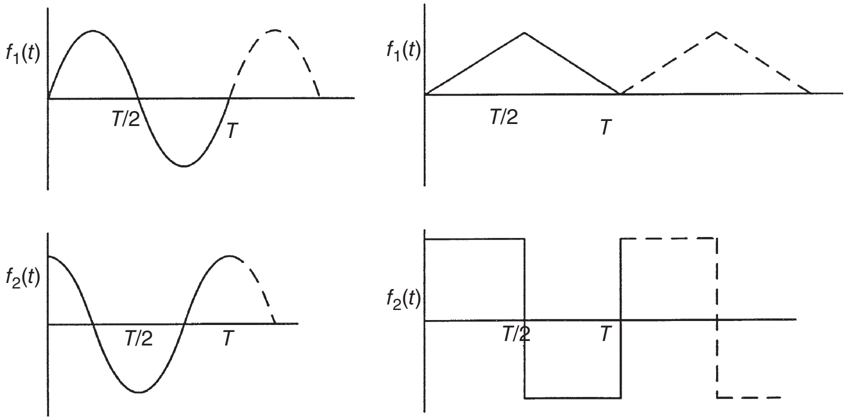

Figure 2.2 Orthogonal functions.

Nonzero values occur when $m = n$:

$$\int_0^T \sin^2 m\omega_0 t\, dt = T/2 \quad \text{all } m$$

$$\int_0^T \cos^2 m\omega_0 t\, dt = T/2 \quad \text{all } n \tag{2.6}$$

2.3 FOURIER SERIES AND COEFFICIENTS

A periodic function can be expanded in a Fourier series. The series has the expression:

$$f(t) = a_0 + \sum_{n=1}^{\infty} \left(a_n \cos\left(\frac{2\pi nt}{T}\right) + b_n \sin\left(\frac{2\pi nt}{T}\right)\right) \tag{2.7}$$

where a_0 is the average value of function $f(t)$. It is also called the DC component, and a_n and b_n are called the coefficients of the series. A series such as Eq. (2.7) is called a trigonometric Fourier series. The Fourier series of a periodic function is the sum of sinusoidal components of different frequencies. The term $2\pi/T$ can be written as ω. The nth term $n\omega$ is then called the nth harmonic and $n = 1$ gives the fundamental; a_0, a_n, and b_n are calculated as follows:

$$a_0 = \frac{1}{T}\int_{-T/2}^{T/2} f(t)dt \tag{2.8}$$

$$a_n = \frac{2}{T}\int_{-T/2}^{T/2} \cos\left(\frac{2\pi nt}{T}\right) dt \qquad \text{for } n = 1, 2, \ldots, \infty \tag{2.9}$$

$$b_n = \frac{2}{T}\int_{-T/2}^{T/2} \sin\left(\frac{2\pi nt}{T}\right)dt \qquad \text{for } n = 1, 2, \ldots, \infty \tag{2.10}$$

These equations can be written in terms of angular frequency:

$$a_0 = \frac{1}{2\pi}\int_{-\pi}^{\pi} f(x)\,\omega t \mathrm{d}\omega t \tag{2.11}$$

$$a_n = \frac{1}{\pi}\int_{-\pi}^{\pi} f(x)\,\omega t\ \cos(n\omega t)\,\mathrm{d}\omega t \tag{2.12}$$

$$b_n = \frac{1}{\pi}\int_{-\pi}^{\pi} f(x)\,\omega t \sin(n\omega t)\,\mathrm{d}\omega t \tag{2.13}$$

This gives

$$x(t) = a_0 + \sum_{n=1}^{\infty}[a_n\ \cos(n\omega t) + b_n\ \sin(n\omega t)] \tag{2.14}$$

We can write

$$\begin{aligned} a_n\ \cos n\omega t + b_n\ \sin \omega t &= [a_n^2 + b_n^2]^{1/2}[\sin \phi_n\ \cos n\omega t + \cos \phi_n\ \sin n\omega t] \\ &= [a_n^2 + b_n^2]^{1/2}\ \sin(n\omega t + \phi_n) \end{aligned} \tag{2.15}$$

where

$$\phi_n = \tan^{-1}\frac{a_n}{b_n}$$

The coefficients can be written in terms of two separate integrals:

$$\begin{aligned} a_n &= \frac{2}{T}\int_0^{T/2} x(t)\cos\left(\frac{2\pi nt}{T}\right)dt + \frac{2}{T}\int_{-T/2}^{0} x(t)\cos\left(\frac{2\pi nt}{T}\right)dt \\ b_n &= \frac{2}{T}\int_0^{T/2} x(t)\sin\left(\frac{2\pi nt}{T}\right)dt + \frac{2}{T}\int_{-T/2}^{0} x(t)\sin\left(\frac{2\pi nt}{T}\right)dt \end{aligned} \tag{2.16}$$

Example 2.1: Find the Fourier series of a periodic function of period 1 defined by

$$\begin{aligned} f(x) &= 1/2 + x, \quad -1/2 < x \le 0 \\ &= 1/2 - x, \quad 0 < x < 1/2 \end{aligned}$$

When the period of the function is not 2π, it is converted to length 2π, and the independent variable is also changed proportionally. Say, if the function is defined in interval $(-t,\ t)$, then 2π is interval for the variable $= \pi x/t$, so put $z = \pi x/t$ or $x = zt/\pi$. The function $f(x)$ of $2t$ is transformed to function $f(tz/\pi)$ or $F(z)$ of 2π. Let

$$f(x) = \frac{a_0}{2} + a_1\ \cos\frac{\pi x}{t} + a_2\ \cos\frac{2\pi x}{t} + \ldots . b_1\ \sin\frac{\pi x}{t} + a_2\ \sin\frac{2\pi x}{t} + \ldots .$$

$$2t = 1$$

By definition,

$$a_0 = \frac{1}{1/2}\int_{-1/2}^{0}\left(\frac{1}{2}+x\right)dx + \frac{1}{1/2}\int_{0}^{1/2}\left(\frac{1}{2}-x\right)dx = 1/2$$

$$a_n = \frac{1}{t}\int_{-t}^{t} f(x)\cos\frac{n\pi x}{t}\,dx$$

$$= \frac{1}{1/2}\int_{-1/2}^{0}\left(\frac{1}{2}+x\right)\cos\frac{n\pi x}{1/2}dx + \int_{0}^{1/2}\left(\frac{1}{2}-x\right)\cos\frac{n\pi x}{1/2}dx$$

$$= 2\left[\left(\frac{1}{2}+x\right)\frac{\sin 2n\pi x}{2n\pi} - (1)\left(\frac{\cos 2n\pi x}{4n^2\pi^2}\right)\right]_{-1/2}^{0}$$

$$+\, 2\left[\left(\frac{1}{2}-x\right)\frac{\sin 2n\pi x}{2n\pi} - (-1)\left(\frac{-\cos 2n\pi x}{4n^2\pi^2}\right)\right]_{0}^{1/2}$$

$$= \frac{2}{n^2\pi^2} \quad \text{for} \quad n = \text{odd}$$

$$= 0 \qquad \text{for} \quad n = \text{even}$$

$$b_n = \frac{1}{t}\int_{-t}^{t} f(x)\sin\frac{n\pi x}{t}\,dx$$

$$= \frac{1}{1/2}\int_{-1/2}^{0}\left(\frac{1}{2}+x\right)\sin\frac{n\pi x}{1/2}dx + \int_{0}^{1/2}\left(\frac{1}{2}-x\right)\sin\frac{n\pi x}{1/2}dx$$

$$= 2\left[\left(\frac{1}{2}+x\right)\frac{-\cos 2n\pi x}{2n\pi} - (1)\left(-\frac{\sin 2n\pi x}{4n^2\pi^2}\right)\right]_{-1/2}^{0}$$

$$+\, 2\left[\left(\frac{1}{2}-x\right)\frac{-\cos 2n\pi x}{2n\pi} - (-1)\left(\frac{-\sin 2n\pi x}{4n^2\pi^2}\right)\right]_{0}^{1/2} = 0$$

Substituting the values

$$f(x) = \frac{1}{4} + \frac{2}{\pi^2}\left[\frac{\cos 2\pi x}{1^2} + \frac{\cos 6\pi x}{3^2} + \frac{\cos 10\pi x}{5^2} - \ldots.\right]$$

2.4 ODD SYMMETRY

A function $f(x)$ is said to be an odd or skew symmetric function, if

$$f(-x) = -f(x) \tag{2.17}$$

The area under the curve from $-T/2$ to $T/2$ is zero. This implies that

$$a_0 = 0, a_n = 0 \tag{2.18}$$

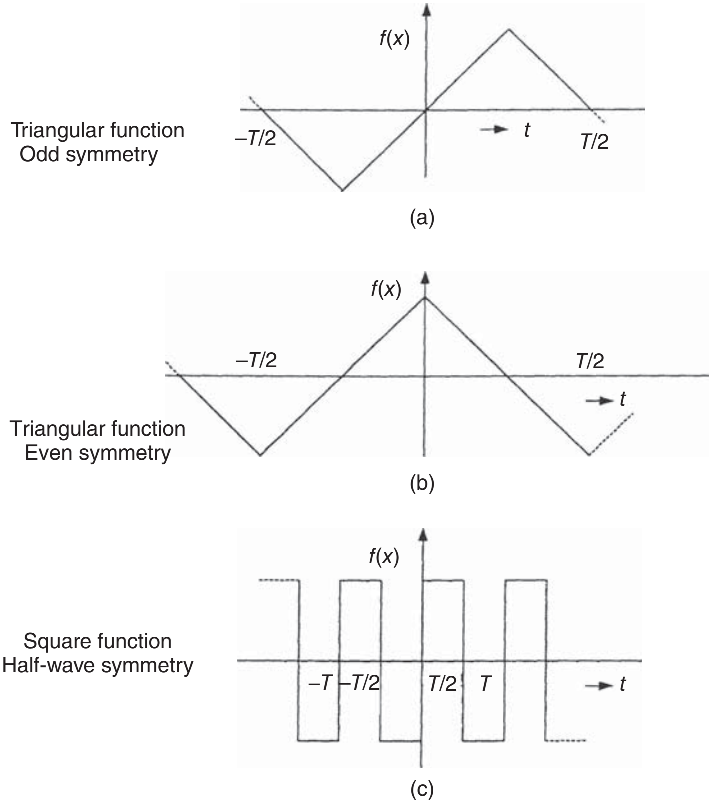

Figure 2.3 (a) Triangular function with odd symmetry, (b) triangular function with even symmetry, and (c) square function with half-wave symmetry.

$$b_n = \frac{4}{T}\int_0^{T/2} f(t)\sin\left(\frac{2\pi nt}{T}\right)dt \tag{2.19}$$

Figure 2.3(a) shows a triangular function, having odd symmetry, the Fourier series contains only sine terms.

2.5 EVEN SYMMETRY

A function $f(x)$ is even symmetric, if

$$f(-x) = f(x) \tag{2.20}$$

The graph of such a function is symmetric with respect to the y-axis. The y-axis is a mirror reflection of the curve.

$$a_0 = 0, b_n = 0 \tag{2.21}$$

$$a_n = \frac{4}{T}\int_0^{T/2} f(t)\cos\left(\frac{2\pi nt}{T}\right)dt \tag{2.22}$$

Figure 2.3(b) shows a triangular function with even symmetry. The Fourier series contains only cosine terms. Note that the odd and even symmetry has been obtained with the triangular function by shifting the origin.

2.6 HALF-WAVE SYMMETRY

A function is said to have half-wave symmetry if

$$f(x) = -f(x + T/2) \tag{2.23}$$

Figure 2.3(c) shows that a square-wave function has half-wave symmetry, with respect to the period $-T/2$. The negative half-wave is the mirror image of the positive half, but phase shifted by $T/2$ (or π radians). Due to half-wave symmetry, the average value is zero. The function contains only odd harmonics.

If n is odd, then

$$a_n = \frac{4}{T}\int_0^{T/2} x(t)\cos\left(\frac{2\pi nt}{T}\right)dt \tag{2.24}$$

and $a_n = 0$ for $n =$ even.

$$b_n = \frac{4}{T}\int_0^{T/2} x(t)\sin\left(\frac{2\pi nt}{T}\right)dt \tag{2.25}$$

for $n =$ odd, and it is zero for $n =$ even.

Example 2.2: Calculate the Fourier series for an input current to a six-pulse converter, with a firing angle of α.

Then, as the wave is symmetrical, DC component is zero.

The waveform pattern with firing angle α is shown in Fig. 2.4.

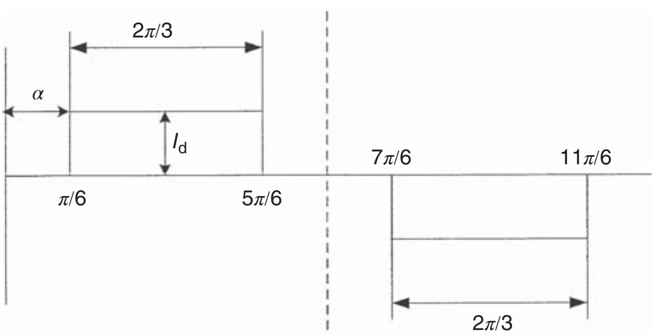

Figure 2.4 Waveform for Example 2.2.

The Fourier series of the input current is

$$\sum_{n=1}^{\infty}(a_n \cos n\omega t + b_n \sin n\omega t)$$

$$a_n = \frac{1}{\pi}\left[\int_{\pi/6+\alpha}^{5\pi/6+\alpha} I_d \cos n\omega t \; d(\omega t) - \int_{7\pi/6+\alpha}^{11\pi/6+\alpha} I_d \cos n\omega t \; d(\omega t)\right]$$

$$= -\frac{4I_d}{n\pi}\sin\frac{n\pi}{3}\sin n\alpha, \quad \text{for} \quad n = 1, 3, 5, \ldots$$

$$= 0, \quad \text{for } n = 2, 6, \ldots$$

$$b_n = \frac{1}{\pi}\left[\int_{\pi/6+\alpha}^{5\pi/6+\alpha} I_d \sin n\omega t \; d(\omega t) - \int_{7\pi/6+\alpha}^{11\pi/6+\alpha} I_d \sin n\omega t \; d(\omega t)\right]$$

$$= \frac{4I_d}{n\pi}\sin\frac{n\pi}{3}\cos n\alpha \quad \text{for} \quad n = 1, 3, 5..$$

$$= 0, \text{ for } \quad n = \text{even}$$

We can write the Fourier series as

$$i = \sum_{n=1,2,..}^{\infty} \sqrt{2}I_n \sin(n\omega t + \phi_n)$$

where i is the instantaneous current and

$$\phi_n = \tan^{-1}\frac{a_n}{b_n} = -n\alpha$$

Rms value of nth harmonic is

$$I_{n,\text{rms}} = \frac{1}{\sqrt{2}}(a_n^2 + b_n^2)^{1/2}$$

$$= \frac{2\sqrt{2}I_d}{n\pi}\sin\frac{n\pi}{3}$$

The fundamental rms current is

$$I_1 = \frac{\sqrt{6}}{\pi}I_d = 0.7797I_d$$

Example 2.3: A single-phase full bridge supplies a motor load. Assuming that the motor DC current is ripple free, determine the input current (using Fourier analysis), harmonic factor, distortion factor, and power factor for an ignition delay angle of α.

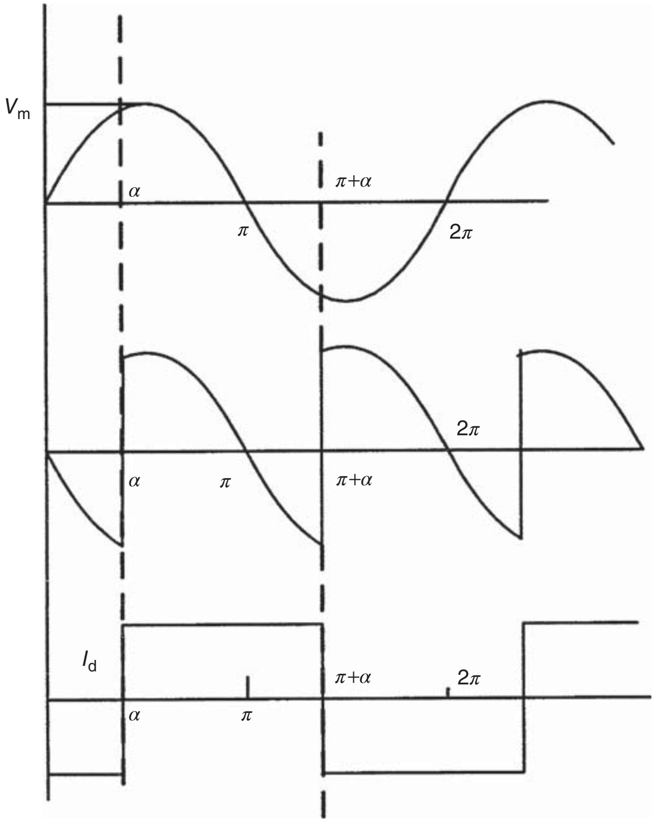

Figure 2.5 Waveforms of fully controlled single-phase bridge (Example 2.3).

The waveform of full-wave single-phase bridge rectifier is shown in Fig. 2.5. The average value of DC voltage is

$$V_{\mathrm{DC}} = \int_{\alpha}^{\pi+\alpha} V_m \sin \omega t \; d(\omega t)$$

$$= \frac{2V_m}{\pi} \cos \alpha$$

It can be controlled by change of conduction angle α.

From Fig. 2.5, the instantaneous input current can be expressed in the Fourier series as

$$I_{\mathrm{input}} = I_{\mathrm{DC}} + \sum_{n=1,2,\ldots}^{\infty} (a_n \cos n\omega t + b_n \sin n\omega t)$$

$$I_{\mathrm{DC}} = \frac{1}{2\pi} \int_{\alpha}^{2\pi+\alpha} i(t) d(\omega t) = \frac{1}{\pi} \left[\int_{\alpha}^{\pi+\alpha} I_a d\,(\omega t) + \int_{\pi+\alpha}^{2\pi+\alpha} I_a d(\omega t) \right] = 0$$

Also

$$a_n = \frac{1}{\pi}\int_{\alpha}^{2\pi+\alpha} i(t)\cos n\omega t \;\, d(\omega t)$$
$$= -\frac{4I_a}{n\pi}\sin n\alpha \quad \text{for } \; n = 1, 3, 5$$
$$= 0 \quad \text{for } \; n = 2, 4, ...$$
$$b_n = \frac{1}{\pi}\int_{\alpha}^{2\pi+\alpha} i(t)\sin n\omega t \;\, d(\omega t)$$
$$= \frac{4I_a}{n\pi}\cos n\alpha \quad \text{for } \; n = 1, 3, 5$$
$$= 0 \quad \text{for } \; n = 2, 4, ...$$

We can write the instantaneous input current as

$$i_{\text{input}} = \sum_{n=1,2,\ldots}^{\infty} \sqrt{2}I_n \;\sin(\omega t + \phi_n)$$

where

$$\phi_n = \tan^{-1}\left(\frac{a_n}{b_n}\right) = -n\alpha$$

$\phi_n = -n\alpha$ is the displacement angle of the *n*th harmonic current. The rms value of the *n*th harmonic input current is

$$I_n = \frac{1}{\sqrt{2}}(a_n^2 + b_n^2)^{1/2} = \frac{2\sqrt{2}}{n\pi}I_a$$

The rms value of the fundamental current is

$$I_1 = \frac{2\sqrt{2}}{\pi}I_d$$

Thus, the rms value of the input current is

$$I_{\text{rms}} = \left(\sum_{n=1}^{\infty} I_n^2\right)^{1/2}$$

The harmonic factor is

$$\text{HF} = \left[\left(\frac{I_{\text{rms}}}{I_1}\right)^2 - 1\right]^{1/2} = 0.4834$$

The displacement factor is

$$\mathrm{DF} = \cos\phi_1 = \cos(-\alpha)$$

The power factor is

$$\mathrm{PF} = \frac{V_{\mathrm{rms}} I_1}{V_{\mathrm{rms}} I_{\mathrm{rms}}} \cos\phi_1 = \frac{2\sqrt{2}}{\pi}\cos\alpha$$

2.7 HARMONIC SPECTRUM

The Fourier series of a square-wave function is

$$f(t) = \frac{4k}{\pi}\left(\frac{\sin\omega t}{1} + \frac{\sin 3\omega t}{3} + \frac{\sin 5\omega t}{5} + \cdots\right) \tag{2.26}$$

where k is the amplitude of the function. The magnitude of the nth harmonic is $1/n$, when the fundamental is expressed as one per unit.

The construction of a square wave from the component harmonics is shown in Fig. 2.6(a), and the plotting of harmonics as a percentage of the magnitude of the fundamental gives the harmonic spectrum of Fig. 2.6(b). A harmonic spectrum indicates the relative magnitude of the harmonics with respect to the fundamental and is not indicative of the sign (positive or negative) of the harmonic nor its phase angle.

2.8 COMPLEX FORM OF FOURIER SERIES

A vector with amplitude A and phase angle θ with respect to a reference can be resolved into two oppositely rotating vectors of half the magnitude so that

$$|A|\cos\theta = |A/2|e^{j\theta} + |A/2|e^{-j\theta} \tag{2.27}$$

Thus,

$$a_n \cos n\omega t + b_n \sin n\omega t \tag{2.28}$$

can be substituted by

$$\cos(n\omega t) = \frac{e^{jn\omega t} + e^{-jn\omega t}}{2} \tag{2.29}$$

$$\sin(n\omega t) = \frac{e^{jn\omega t} - e^{-jn\omega t}}{2j} \tag{2.30}$$

Thus,

$$x(t) = \frac{a_0}{2} + \frac{1}{2}\sum_{n=1}^{n=\infty}(a_n - jb_n)e^{jn\omega t} + \frac{1}{2}\sum_{n=1}^{n=\infty}(a_n - jb_n)e^{-jn\omega t} \tag{2.31}$$

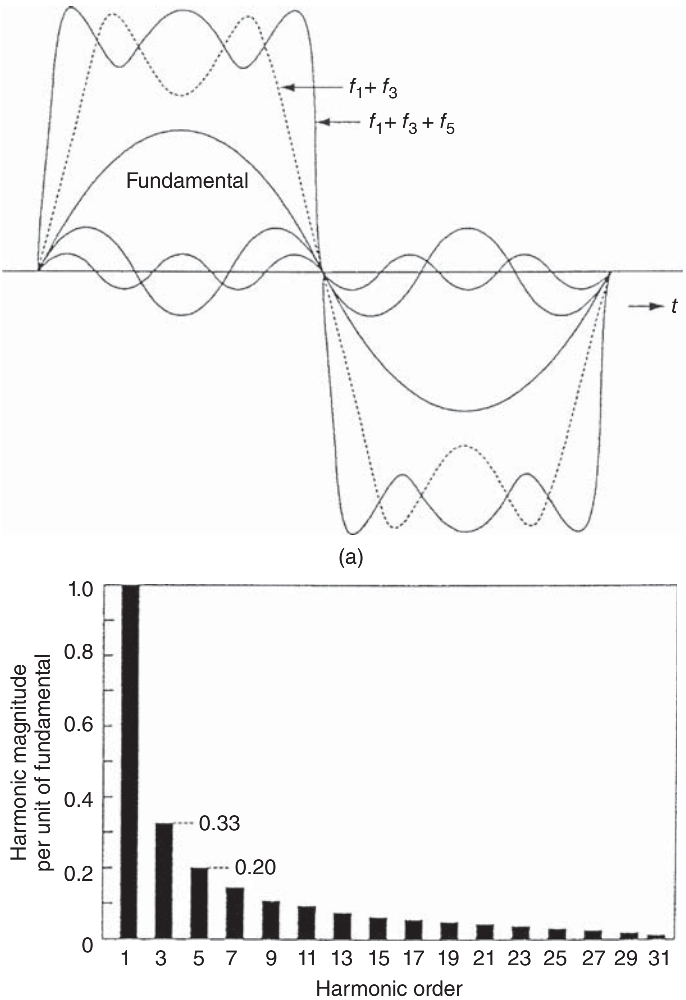

(b)

Figure 2.6 (a) Construction of a square wave from its harmonic components and (b) harmonic spectrum.

We introduce negative values of n in the coefficients, that is,

$$a_{-n} = \frac{2}{T}\int_{-T/2}^{T/2} x(t)\cos(-n\omega t)\mathrm{d}t = \frac{2}{T}\int_{-T/2}^{T/2} x(t)\cos(n\omega t)\mathrm{d}t = a_n \quad n = 1, 2, 3, \ldots \tag{2.32}$$

$$b_{-n} = \frac{2}{T}\int_{-T/2}^{T/2} x(t)\sin(-n\omega t)dt = -\frac{2}{T}\int_{-T/2}^{T/2} x(t)\sin(n\omega t)dt = -b_n \quad n = 1, 2, 3, \ldots \tag{2.33}$$

Hence,

$$\sum_{n=1}^{\infty} a_n e^{-jn\omega t} = \sum_{n=-1}^{\infty} a_n e^{jn\omega t} \tag{2.34}$$

and

$$\sum_{n=1}^{\infty} jb_n e^{-jn\omega t} = \sum_{n=-1}^{\infty} jb_n e^{jn\omega t} \tag{2.35}$$

Therefore, substituting in Eq. (2.31), we obtain

$$x(t) = \frac{a_0}{2} + \frac{1}{2}\sum_{n=-\infty}^{\infty} (a_n - jb_n)e^{jn\omega t} = \sum_{n=-\infty}^{\infty} c_n e^{jn\omega t} \tag{2.36}$$

This is the expression for a Fourier series expressed in exponential form, which is the preferred approach for analysis. The coefficient c_n is complex and is given by

$$c_n = \frac{1}{2}(a_n - jb_n) = \frac{1}{T}\int_{-T/2}^{T/2} x(t)e^{-jn\omega t}\mathrm{d}t \quad n = 0, \pm 1, \pm 2, \ldots \tag{2.37}$$

2.9 FOURIER TRANSFORM

Fourier analysis of a continuous periodic signal in the time domain gives a series of discrete frequency components in the frequency domain. The Fourier integral is defined by the expression:

$$X(f) = \int_{\infty}^{-\infty} x(t)e^{-j2\pi ft}dt \tag{2.38}$$

If the integral exists for every value of parameter f (frequency), then this equation describes the Fourier transform. The Fourier transform is a complex quantity:

$$X(f) = R(f) + jI(f) = |X(f)|e^{j\phi(f)} \tag{2.39}$$

where $R(f)$ is the real part of the Fourier transform and $I(f)$ is the imaginary part of the Fourier transform. The amplitude or *Fourier spectrum of* $x(t)$ is given by

$$|X(f)| = \sqrt{R^2(f) + I^2(f)} \tag{2.40}$$

The phase angle of the Fourier transform is given by

$$\phi(f) = \tan^{-1}\frac{I(f)}{R(f)} \tag{2.41}$$

The inverse Fourier transform or the backward Fourier transform is defined as

$$x(t) = \int_{-\infty}^{\infty} X(f)e^{j2\pi ft}df \tag{2.42}$$

Inverse transformation allows determination of a function in time domain from its Fourier transform. Equations (2.38) and (2.42) are a Fourier transform pair, and the relationship can be indicated by

$$x(t) \leftrightarrow X(f) \tag{2.43}$$

Fourier transform pair is also written as

$$X(w) = a_1 \int_{-\infty}^{\infty} x(t)e^{-j\omega t}dt$$

$$x(t) = a_2 \int_{-\infty}^{\infty} X(\omega)e^{j\omega t}d\omega$$

where a_1 and a_2 can take different values depending on the user, some take $a_1 = 1$ and $a_2 = 1/2\pi$, or set $a_1 = 1/2\pi$ and $a_2 = 1$ or $a_1 = a_2 = 1/\sqrt{2\pi}$. The requirement is that $a_1 \times a_2 = 1/2\pi$. In most texts, it is defined as

$$X(w) = \int_{-\infty}^{\infty} x(t)e^{-j\omega t}dt$$

$$x(t) = \frac{1}{2\pi}\int_{-\infty}^{\infty} X(\omega)e^{j\omega t}d\omega$$

However, definitions in equations (2.38) and (2.42) are consistent with Laplace transform.

Example 2.4: Consider a function defined as

$$\begin{aligned} x(t) &= \beta e^{-\alpha t} t > 0 \\ &= 0 \ \ t < 0 \end{aligned} \tag{2.44}$$

It is required to write its forward Fourier transform.

From Eq. (2.38),

$$\begin{aligned} X(f) &= \int_{0}^{\infty} \beta e^{-\alpha t}e^{-j2\pi ft}\mathrm{d}t \\ &= \frac{-\beta}{\alpha + j2\pi f}e^{-(\alpha+j2\pi f)t}\Big|_0^{\infty} \\ &= \frac{\beta}{\alpha + j2\pi f} = \frac{\beta\alpha}{\alpha^2 + (2\pi f)^2} - j\frac{2\pi f\beta}{\alpha^2 + (2\pi f)^2} \end{aligned}$$

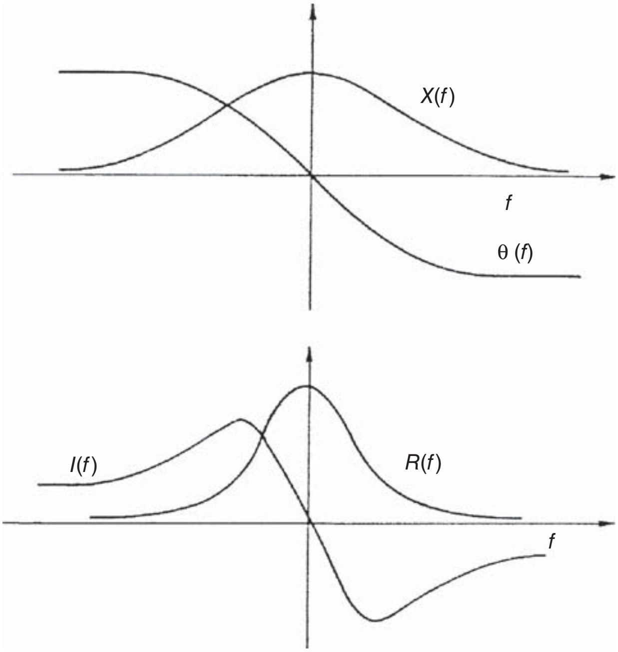

Figure 2.7 Real, imaginary, magnitude, and phase angle representations of the Fourier transform (Example 2.5).

$$R(f) = \frac{\beta\alpha}{\alpha^2 + (2\pi f)^2}$$

$$I(f) = -j\frac{2\pi f\beta}{\alpha^2 + (2\pi f)^2}$$

Thus, $X(f)$ is

$$\frac{\beta}{\sqrt{\alpha^2 + (2\pi f)^2}} e^{j\,\tan^{-1}[-2\pi f/\alpha]} \tag{2.45}$$

This is plotted in Fig. 2.7.

Example 2.5: Convert the function arrived at in Example 2.4 to $x(t)$.

The inverse Fourier transform is

$$\begin{aligned} x(t) &= \int_{-\infty}^{\infty} X(f) e^{j2\pi ft}\, df \\ &= \int_{-\infty}^{\infty} \left[\frac{\beta\alpha}{\alpha^2 + (2\pi f)^2} - j\frac{2\pi f\beta}{\alpha^2 + (2\pi f)^2}\right] e^{j2\pi ft}\, df \end{aligned}$$

$$= \int_{-\infty}^{\infty} \left[\frac{\beta\alpha \cos(2\pi ft)}{\alpha^2 + (2\pi f)^2} + \frac{2\pi f \beta \sin(2\pi ft)}{\alpha^2 + (2\pi f)^2} \right] df$$

$$+ j \int_{-\infty}^{\infty} \left[\frac{\beta\alpha \sin(2\pi ft)}{\alpha^2 + (2\pi f)^2} + \frac{2\pi f \beta \cos(2\pi ft)}{\alpha^2 + (2\pi f)^2} \right] df$$

The imaginary term is zero, as it is an odd function.

This can be written as

$$x(t) = \frac{\beta\alpha}{(2\pi)^2} \int_{-\infty}^{\infty} \frac{\cos(2\pi tf)}{(\alpha/2\pi)^2 + f^2} df + \frac{2\pi\beta}{(2\pi)^2} \int_{-\infty}^{\infty} \frac{f \ \sin(2\pi tf)}{(\alpha/2\pi)^2 + f^2} df$$

As

$$\int_{-\infty}^{\infty} \frac{\cos \alpha x}{b^2 + x^2} dx = \frac{\pi}{b} e^{-ab}$$

and

$$\int_{-\infty}^{\infty} \frac{x \ \sin ax}{b^2 + x^2} dx = \pi e^{-ab}$$

$x(t)$ becomes

$$x(t) = \frac{\beta\alpha}{(2\pi)^2} \left[\frac{\pi}{\alpha/2\pi} \mathrm{e}^{-(2\pi t)(\alpha/2\pi)} \right] + \frac{2\pi\beta}{(2\pi)^2} [\pi e^{-(2\pi t)(\alpha/2\pi)}]$$

$$= \frac{\beta}{2} e^{-\alpha t} + \frac{\beta}{2} \mathrm{e}^{-\alpha t} = \beta \mathrm{e}^{-\alpha t} \ t > 0$$

that is,

$$\beta \mathrm{e}^{-\alpha t} t > 0 \leftrightarrow \frac{\beta}{\alpha + j2\pi f} \tag{2.46}$$

Example 2.6: Consider a function defined by

$$x(t) = K; \text{for } |t| \le T/2$$
$$= 0; \text{for } |t| > T/2 \tag{2.47}$$

It is a bandwidth limited rectangular function (Fig. 2.8(a)); the Fourier transform is

$$X(f) = \int_{-T/2}^{T/2} K \mathrm{e}^{-j2\pi fT} dt = KT \left[\frac{\sin(\pi fT)}{\pi fT} \right] \tag{2.48}$$

The term in parentheses in Eq. (2.48) is called the *sinc function.* The function has zero value at points $f = n/T$. Figure 2.8(b) shows zeros and side lobes.

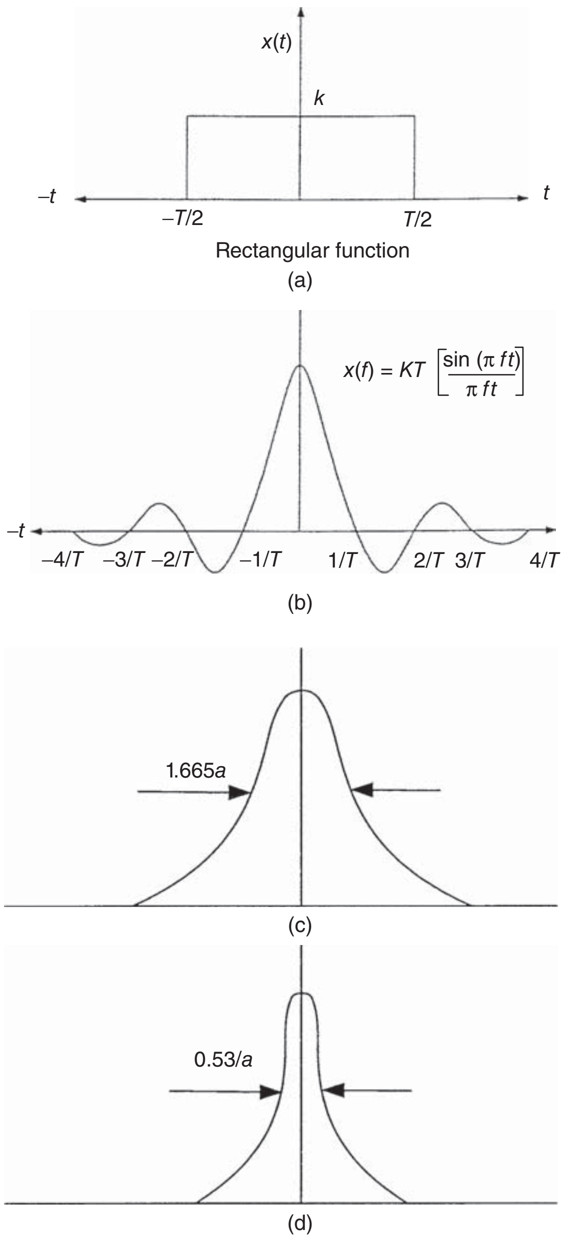

Figure 2.8 (a) Bandwidth limited rectangular function, (b) the sinc function showing side lobes, and (c) and (d) a Gaussian function with its transform.

2.9.1 Fourier Transform of Some Common Functions

Gaussian Function Consider the function:

$$x(t) = e^{-x^2/a^2} \tag{2.49}$$

where a is the width parameter. The value of $x(t) = 1/2$ when $(x/a)^2 = \log_e 2$ or $x = \pm 0.9325a$, so that the full width at half maximum (FWHM) = 1.655a. It is shown in Fig. 2.8(c).

$$X(f) = \int_{-\infty}^{\infty} e^{-x^2/a^2} e^{-j2\pi ft} dx$$
$$= a\sqrt{\pi} e^{-\pi^2 a^2 f^2}$$

The Fourier transform is another Gaussian function with width $1/(\pi a)$.

Note that the original function has a width of $1.665a$ at half maximum. The Fourier transform has a narrower width (Fig. 2.8(d)).

Some Common Transforms Figure 2.9 (a–j) shows graphically the Fourier transforms of some common functions.

The following transforms exist:

(a) Fourier transformer of an impulse function:

$$x(t) = K\delta(t)$$
$$X(f) = K \tag{2.50}$$

This means that the Fourier transform of a delta function is unity.

$$\delta(t) \leftrightarrow 1 \tag{2.51}$$

For a pair of delta functions, equally placed on either side of the origin, the Fourier transform is a cosine wave:

$$\delta(t-a)\delta(t-a) = e^{j2\pi fa} + e^{-j2\pi fa}$$
$$= 2\ \cos(2\pi fa) \tag{2.52}$$

(b) Fourier transform of a constant amplitude waveform:

$$x(t) = K$$
$$X(f) = K\delta(f) \tag{2.53}$$

(c) Fourier transform of a pulse waveform:

$$x(t) = A \quad |t| < T_0$$
$$= (A/2) \quad |t| = T_0$$
$$= 0 \quad |t| > T_0$$
$$X(f) = 2AT_0 \frac{\sin(2\pi T_0 f)}{2\pi T_0 f} \tag{2.54}$$

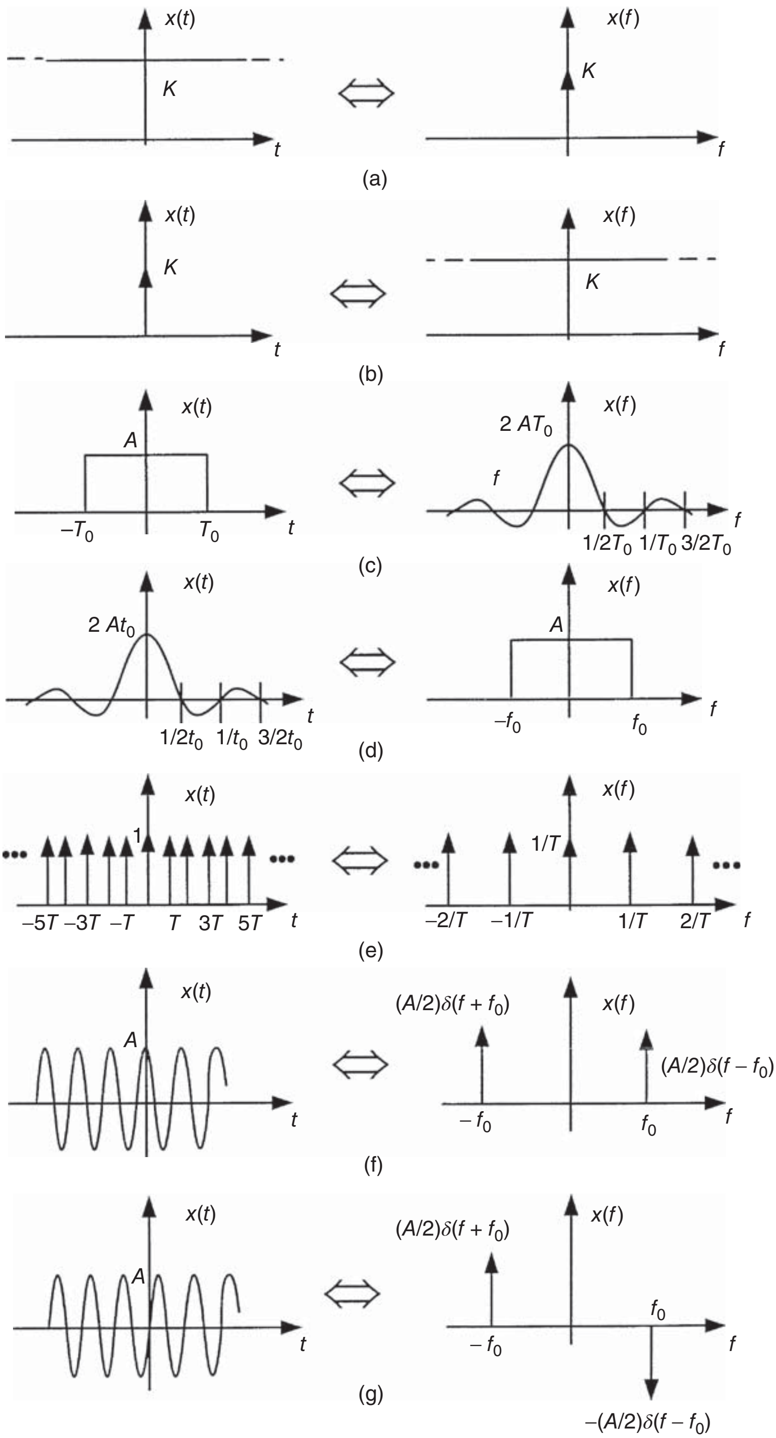

Figure 2.9 (a–j) Fourier transforms of some common functions.

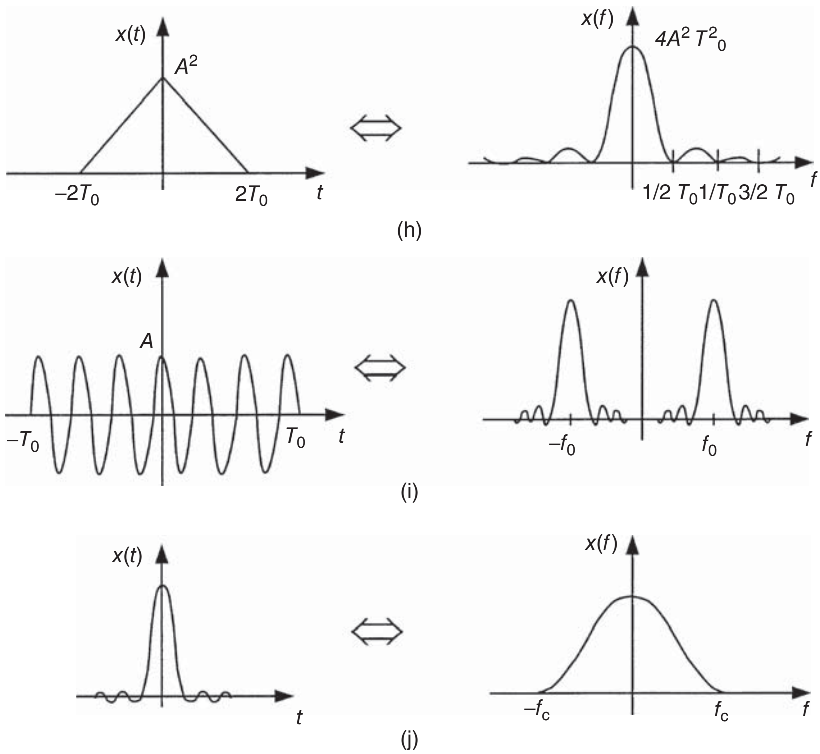

Figure 2.9 (*Continued*)

(d) This represents situation in reverse.

(e) The Fourier transform of sequence of equal distance pulses is another sequence of equal distance pulses.

$$x(t) = \sum_{n=-\infty}^{\infty} \delta(t - nT)$$

$$X(f) = \frac{1}{T}\sum_{n=-\infty}^{\infty} \delta\left(f - \frac{n}{T}\right) \tag{2.55}$$

(f), (g) Fourier transform of periodic functions

$$x(t) = A\ \cos(2\pi f_0 t)$$

$$X(f) = \frac{A}{2}\delta(f - f_0) + \frac{A}{2}\delta(f + f_0)$$

$$x(t) = A\ \sin(2\pi f_0 t)$$

$$X(f) = -j\frac{A}{2}\delta(f - f_0) + j\frac{A}{2}\delta(f + f_0) \tag{2.56}$$

(h) Fourier transform of triangular function:

$$x(t) = A^2 - \frac{A^2}{2T_0}$$

$$= 0 \quad |t| < \ 2T_0$$

$$= 0 \quad |t| > 2T_0$$

$$X(f) = A^2 \frac{\sin^2(2\pi T_0 f)}{(\pi f)^2} \tag{2.57}$$

(i) Fourier transform of

$$x(t) = A\ \cos(2\pi f_0 t) \quad |t| < T_0$$

$$= 0 \qquad\qquad |t| > T_0$$

$$X(f) = A^2 T_0 \left[\frac{\sin(2\pi T_0 f}{2\pi T_0 f}\left(f + f_0\right) + \frac{\sin(2\pi T_0 f}{2\pi T_0 f}(f - f_0)\right] \tag{2.58}$$

(j) Fourier transform of

$$x(t) = \frac{1}{2}q(t) + \frac{1}{4}q\left(t + \frac{1}{2f_c}\right) + \frac{1}{4}q\left(t - \frac{1}{2f_c}\right)$$

where

$$q(t) = \frac{\sin(2\pi f_c t)}{\pi t}$$

$$X(f) = \frac{1}{2} + \frac{1}{2}\cos\left(\frac{\pi f}{f_c}\right) \quad |f| \le f_c$$

$$= 0 \qquad\qquad |f| > f_c \tag{2.59}$$

(k) Fourier transform of Dirac comb. A Dirac comb is a set of equally spaced δ functions, usually denoted by Cyrillic letter III

$$\mathrm{III}_a(t) = \sum_{n=-\infty}^{\infty} \delta(t - na) \tag{2.60}$$

The Fourier transform is another Dirac comb:

$$\mathrm{III}_a(t) \Leftrightarrow \frac{1}{a}\mathrm{III}_{1/a}(f) \tag{2.61}$$

2.10 DIRICHLET CONDITIONS

Fourier transforms cannot be applied to all functions. The Dirichlet conditions are

- Functions $X(f)$ and $f(t)$ are square integrable:

$$\int_{-\infty}^{\infty} [X(f)]^2 dx \quad X(f) \to 0 \ \ as \ \ |X| \to \infty \tag{2.62}$$

  This implies that the function is finite. A function shown in Fig. 2.10(a) or (b) does not meet this criterion
- $X(f)$ and $x(t)$ are single valued. The function shown in Fig. 2.10(a) does not meet this criterion. There are three values at point A.
- $X(f)$ and $x(t)$ are piecewise continuous. The functions can be broken into separate pieces, so that these can be isolated discontinuous, any number of times.
- Functions $X(f)$ and $x(t)$ have upper and lower bonds. This is the condition that is *sufficient* but not proved to be *necessary*.

  Mostly the functions do behave so that Dirichlet conditions are fulfilled. Consider the so-called "sign" function shown in Fig. 2.11(a) and defined as

$$\begin{aligned} \mathrm{sgn}(t) &= -1 \quad -\infty < t < 0 \\ &= +1 \quad 0 < t < \infty \end{aligned} \tag{2.63}$$

Divide by 2 and add 1/2 to give a Heavyside step of unit height.

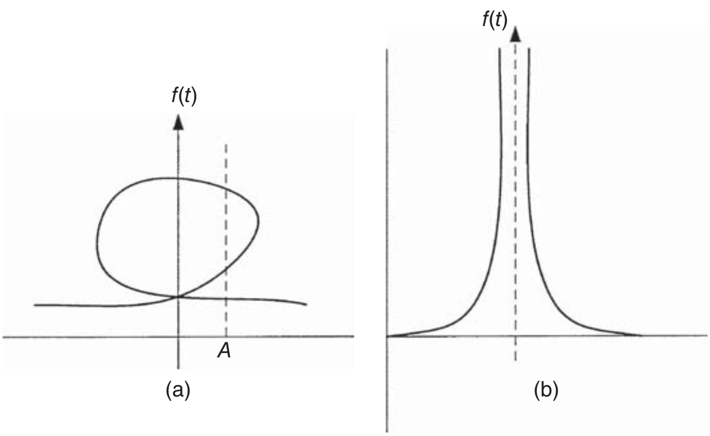

Figure 2.10 (a) A multiple valued function and (b) a discontinuous function.

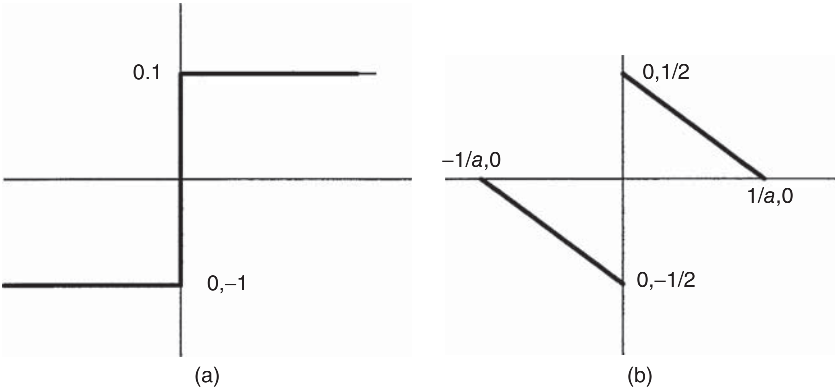

Figure 2.11 (a) A sgn function and (b) representation of a Heavyside step function by two functions that obey Dirichlet constraints.

The function sign(t) / 2 does not obey Dirichlet conditions but can be approximated by considering it as a limiting case of a pair of ramp functions (Fig. 2.11(b))

$$\begin{aligned} x(t) &= \lim_{a\to 0} \frac{-(at+1)}{2} \qquad -1/a < x < 0 \\ &= \lim_{a\to 0} \frac{(1-at)}{2} \quad 0 < x < 1/a \end{aligned} \tag{2.64}$$

A unit step function $u(t)$ can be written in terms of sign function:

$$u(t) = \frac{1}{2} + \frac{1}{2}\mathrm{sgn}(t)$$

Its Fourier transform is

$$\pi\delta(\omega) + \frac{1}{j\omega}$$

Some relations where Dirichlet conditions are applicable are

$$\begin{aligned} X_1(f) + X_2(f) &\leftrightarrow x_1(t) + x_2(t) \\ X(f+a) &\leftrightarrow x(t)e^{j2\pi fa} \\ X(f-a) &\leftrightarrow x(t)e^{-j2\pi fa} \end{aligned} \tag{2.65}$$

Note that if $X(f)$ is a delta function, then

$$\begin{aligned} \delta(X+a) &\leftrightarrow x(t)e^{j2\pi fa} \\ \delta(X-a) &\leftrightarrow x(t)e^{-j2\pi fa} \end{aligned} \tag{2.66}$$

2.11 POWER SPECTRUM OF A FUNCTION

The notion of power spectrum is important in electrical engineering. Consider that the voltage at a point varies with time denoted by $V(t)$. Let $X(f)$ be the Fourier transform of $V(t)$, which can even be negative. Then the power per unit frequency interval being transmitted is proportional to

$$X(f)X(f)^* \tag{2.67}$$

The superscript "*" describes a conjugate. The constant of proportionality depends on load impedance. The function

$$X(f)X(f)^* = |X(f)|^2 \tag{2.68}$$

is called the power spectrum or the spectral power density (SPD) of $V(t)$.

Using equation (2.32), P can be written as

$$P = \frac{1}{T}\int_{-T/2}^{T/2} x^2(t)dt = \frac{1}{T}\int_{-T/2}^{T/2} x(t)(c_n e^{jn\omega t})dt \tag{2.69}$$

Interchanging operation of summation and integration:

$$P = \frac{1}{T}e^{jn\omega t}c_n \int_{-T/2}^{T/2} x(t)(e^{jn\omega t})dt$$

$$= \sum_{n=-\infty}^{\infty} c_n c_{-n}$$

As

$$c_n^* = c_{-n}$$

$$P = \sum_{n=-\infty}^{\infty} |c_n|^2 = |c_0|^2 + 2\sum_{n=1}^{\infty}|F_n|^2 \tag{2.70}$$

This is *Parseval's theorem as applied to exponential Fourier series.* Power in a periodic signal is sum of component powers in exponential Fourier series.

$|c_n|^2$ plotted as a function of $n\omega$ is called power spectrum of $x(t)$

Example 2.7: Fourier series is required for a function of periodic pulse train shown in Fig. 2.12. This can be called a Dirac comb.

From Eq. (2.32),

$$c_n = \frac{1}{T}\int_{-T/2}^{T/2} x(t)e^{-jn\omega t}dt = \frac{Ad}{T}\sin c\left(\frac{n\pi d}{T}\right)$$

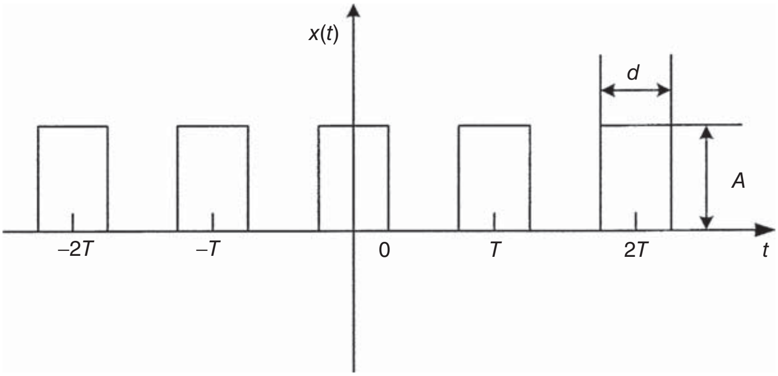

Figure 2.12 A periodic pulse train, Dirac comb.

If $A = 1$, $d = 1/16$, and $T = 1/4$, then

$$c_n = \frac{1}{4} \sin c\left(\frac{n\pi}{4}\right)$$

Thus, Fourier series is given by

$$\sum_{n=-\infty}^{\infty} c_n e^{jn\omega t}$$

The Fourier transform of $x(t)$ is

$$\frac{2\pi Ad}{T} \sum_{n=-\infty}^{\infty} \sin c\left(\frac{n\pi d}{T}\right)\delta(\omega - n\omega_0) \quad \omega_0 = \frac{2\pi}{T}$$

The spectrum has first zero crossing at $n = 4$. The power within first zero crossing is

$$\begin{aligned} P_{n=4} &= |c_0|^2 + 2\{|c_1|^2 + |c_2|^2 + |c_3|^2\} \\ &= \left(\frac{1}{4}\right)^2 + \frac{2}{4^2}\left[\sin c^2\left(\frac{\pi}{4}\right) + \sin c^2\left(\frac{\pi}{2}\right) + \sin c^2\left(\frac{3\pi}{4}\right)\right] \\ &= \frac{1}{16} + \frac{1}{8}(0.811 + 0.405 + 0.090) = 0.226 \end{aligned}$$

The total power of the $x(t)$ is

$$P = \frac{1}{T}\int_{-T/2}^{T/2} x^2(t)dt = \frac{1}{4}\int_{-1/32}^{1/32} 1dt = 0.25$$

2.12 CONVOLUTION

2.12.1 Time Convolution

If

$$x_1(t) \leftrightarrow X_1(\omega)$$
$$x_2(t) \leftrightarrow X_2(\omega) \tag{2.71}$$

then

$$x_1(t) * x_2(t) \leftrightarrow X_1(\omega)X_2(\omega) \tag{2.72}$$

This signifies that convolution in the time domain is multiplication in the frequency domain. Convolution is generally carried out in the frequency domain.

2.12.2 Frequency Convolution

$$x_1(t)x_2(t) \leftrightarrow \frac{1}{2\pi}X_1(\omega) * X_2(\omega) \tag{2.73}$$

Thus, the convolution operation in one domain is transformed to a product operation in the other domain. This has led to the use of transform method, though the time domain is becoming more attractive, for dealing with large dimensional systems. The use of block diagrams and signal flow graphs in the transform domain treats the convolution as an algebraic operator.

The distributive rule:

$$X_1(f) * [X_2(f) + X_3(f)] = X_1(f) * X_2(f) + X_1(f) * X_3(f) \tag{2.74}$$

The commutative rule:

$$X_1(f) * X_2(f) = X_2(f) * X_1(f) \tag{2.75}$$

The associative rule

$$X_1(f) * [X_2(f) * X_3(f)] = [X_1(f) * X_2(f)] * X_3(f) \tag{2.76}$$

Convolution of three functions:

$$X_1(f) * X_2(f) * X_3(f) = \int_{-\infty}^{\infty} \int_{-\infty}^{\infty} X_1(f - f')X_2(f' - f'')df'df'' \tag{2.77}$$

The shift theorem is

$$X(f - a) = X(f) * \delta(t - a) \leftrightarrow x(t)e^{-j2\pi fa} \tag{2.78}$$

Convolution of a pair of δ functions with another function:

$$[\delta(t-a)+\delta(t+a)] * F(X) \leftrightarrow 2\ \cos(2\pi fa)\cdot x(t) \tag{2.79}$$

The convolution of two Gaussian functions is

$$e^{-x^2/a} * e^{-x^2/b} \leftrightarrow ab\pi e^{-\pi^2 f^2 (a^2+b^2)} \tag{2.80}$$

Some relations that can be applied to convolution are

$$[A(f) * B(f)]\cdot[C(f) * D(f)] \leftrightarrow [a(t)\cdot b(t)] * [c(t)\cdot d(t)] \tag{2.81}$$

Note that

$$[A(f) * B(f)]\cdot C(f) \neq A(f) * [B(f)\cdot C(f)] \tag{2.82}$$

$$[A(f) * B(f) + C(f)\cdot D(f)]\cdot E(f) \leftrightarrow [a(t)\cdot b(t) + c(t) * d(t)] * e(t) \tag{2.83}$$

2.12.3 The Convolution Derivative Theorem

The derivative theorem is

$$\frac{dX}{df} \leftrightarrow -j2\pi f x(t) \tag{2.84}$$

Therefore,

$$\frac{d}{df}[X_1(f) * X_2(f)] \leftrightarrow X_1(f) * \frac{dX_2(f)}{df} = \frac{dX_1(f)}{df} * X_2(f) \tag{2.85}$$

Table 2.1 summarizes some properties of Fourier transform, and Table 2.2 gives some useful transform pairs.

2.12.4 Parseval's Theorem

We defined Parseval's theorem in connection with exponential Fourier series. This is also called Rayleigh theorem or simply the power theorem.

$$\int_{-\infty}^{\infty} X_1(f)X_2^*(f)df = \int_{-\infty}^{\infty} f_1(t)f_2^*(t)dt \tag{2.86}$$

2.13 SAMPLED WAVEFORM: DISCRETE FOURIER TRANSFORM

The sampling theorem states that if the Fourier transform of a function $x(t)$ is zero for all frequencies greater than a certain frequency f_c, then the continuous function $x(t)$ can be uniquely determined by a knowledge of the sampled values. The constraint is that $x(t)$ is zero for frequencies greater than f_c, that is, the function is band limited at

TABLE 2.1 Properties of Fourier Transform

Property	Formulation
Linearity	$a_1x_1(t) + a_2x_2(t) \Leftrightarrow a_1X_1(\omega) + a_2X_2(\omega)$
Transformation	$x(t) \Leftrightarrow X(\omega)$
Symmetry	$X(t) \Leftrightarrow 2\pi x(-\omega)$
Scaling	$x(at) \Leftrightarrow (1/\lvert a\rvert)X(\omega/a)$
Delay	$x(t-t_0) \Leftrightarrow e^{-j2\pi f t_0}X(\omega)$
Modulation	$e^{-j2\pi f_0 t}x(t) \Leftrightarrow -X(\omega-\omega_0)$
Time convolution	$x_1(t) * x_2(t) \Leftrightarrow X_1(\omega)X_2(\omega)$
Frequency convolution	$x_1(t)x_2(t) \Leftrightarrow (1/2\pi)X_1(\omega) * X_2(\omega)$
Time differentiation	$\frac{d^n}{dt^n}x(t) \Leftrightarrow (j\omega)^n X(\omega)$
Time integration	$\int_{-\infty}^{t} x(t)dt \Leftrightarrow \frac{X(\omega)}{j\omega} + \pi X(0)\delta(\omega)$
Frequency differentiation	$-jtx(t) \Leftrightarrow \frac{dX(\omega)}{d\omega}$
Frequency integration	$\frac{x(t)}{-jt} \Leftrightarrow \int X(\omega)d\omega$

TABLE 2.2 Some Useful Transforms

$x(t)$	$X(\omega)$
$e^{-at}u(t)$	$\frac{1}{a+j\omega}$
$te^{-at}u(t)$	$\frac{1}{(a+j\omega)^2}$
$\frac{t^{n-1}}{(n-1)!}e^{-at}u(t)$	$\frac{1}{(a+j\omega)^n}$
$\frac{\omega_0}{2\pi}\sin c\left(\frac{\omega_0 t}{2}\right)$	$1, \quad \lvert\omega <\rvert \ \omega_0/2$ $= 0 \quad$ otherwise
$e^{-a\lvert t\rvert}$	$\frac{2a}{a^2+\omega^2}$
$\frac{1}{a^2+t^2}$	$\frac{\pi}{2}e^{-a\lvert\omega\rvert}$
$e^{-at}\ \sin\omega_0 tu(t)$	$\frac{\omega_0}{(a+j\omega)^2+\omega_0^2}$
$e^{-at}\ \cos\omega_0 tu(t)$	$\frac{a+j\omega}{(a+j\omega)^2+\omega_0^2}$
$\sin\omega_0 t$	$j\pi[\delta(\omega+\omega_0) - \delta(\omega-\omega_0)]$
$\cos\omega_0 t$	$\pi[\delta(\omega-\omega_0) + \delta(\omega-\omega_0)]$
$\sum_{n=-\infty}^{\infty} c_n e^{jn\omega_0 t}$	$2\pi\sum_{n=-\infty}^{\infty} c_n\delta(\omega - n\omega_0)$

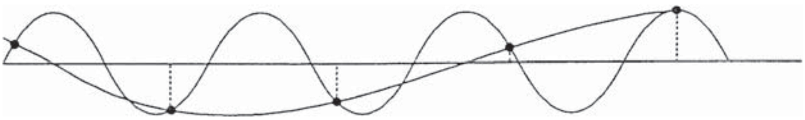

Figure 2.13 High frequency impersonating a low frequency to illustrate aliasing.

frequency f_c. The second constraint is that the sampling spacing must be chosen so that

$$T = 1/(2f_c) \tag{2.87}$$

The frequency $1/T = 2f_c$ is known as the *Nyquist sampling rate.*

Aliasing means that the high-frequency components of a time function can impersonate a low frequency if the sampling rate is low. Figure 2.13 shows a high frequency as well as a low frequency that share identical sampling points. Here, a high frequency is impersonating a low frequency for the same sampling points.

The sampling rate must be high enough for the highest frequency to be sampled at least twice per cycle, $T = 1/(2f_c)$. An input signal $x(t)$ will be represented correctly if this condition is met. The Nyquist frequency is also called *folding frequency*.

Often the functions are recorded as sampled data in the time domain, the sampling being done at a certain frequency. The Fourier transform is represented by the summation of discrete signals where each sample is multiplied by

$$e^{-j2\pi fnt_1} \tag{2.88}$$

that is,

$$X(f) = \sum_{n=-\infty}^{\infty} x(nt_1)e^{-j2\pi fnt_1} \tag{2.89}$$

Figure 2.14 illustrates sampled time domain function and frequency spectrum for a discrete time domain function.

When the frequency domain spectrums as well as the time domain function are sampled functions, the Fourier transform pair is made of discrete components:

$$X(f_k) = \frac{1}{N}\sum_{n=0}^{N-1} x(t_n)e^{-j2\pi kn/N} \tag{2.90}$$

$$X(t_n) = \sum_{k=0}^{N-1} X(f_k)e^{j2\pi kn/N} \tag{2.91}$$

Figure 2.15(a) and (b) shows discrete time and frequency functions. *The discrete Fourier transform* approximates the continuous Fourier transform.

However, errors can occur in the approximations involved. Consider a cosine function $x(t)$ and its continuous Fourier transform $X(f)$, which consists of two impulse functions that are symmetric about zero frequency (Fig. 2.16(a)).

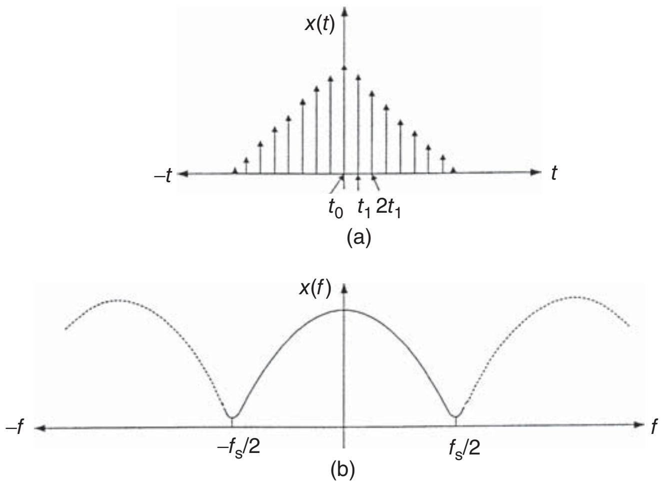

Figure 2.14 (a) Sampled time domain function and (b) frequency spectrum for the time domain function.

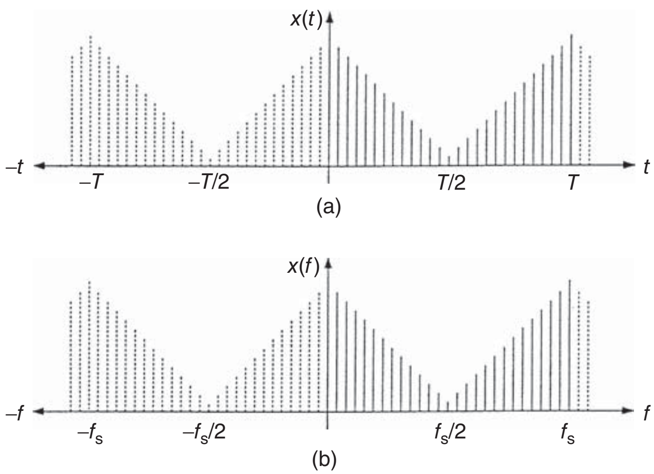

Figure 2.15 (a) and (b) discrete time and frequency domain functions.

The finite portion of $x(t)$, which can be viewed through a unity amplitude window $w(t)$, and its Fourier transform $W(f)$, which has side lobes, are shown in Fig. 2.16(b).

Figure 2.16(c) shows that the corresponding convolution of two frequency signals results in blurring of $X(f)$ into two $\sin x/x = \sin c(x)$ shaped pulses. Thus, the estimate of $X(f)$ is fairly corrupted.

The sampling of $x(t)$ is performed by multiplying with $c(t)$ (Fig. 2.16(d)); the resulting frequency domain function is shown in Fig. 2.16(e).

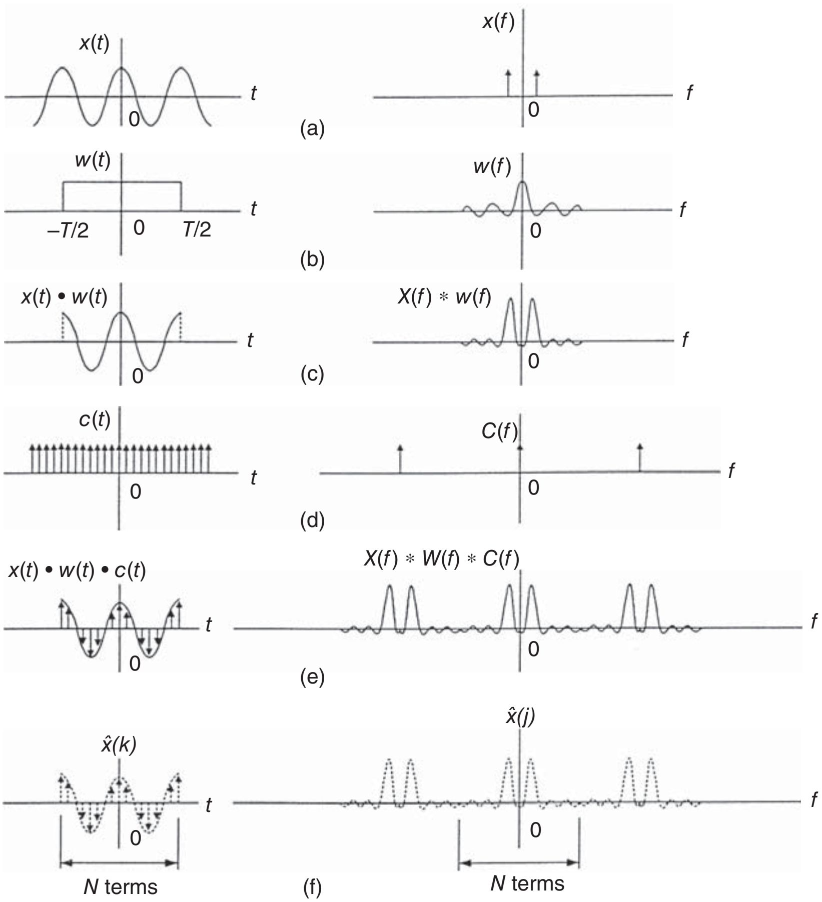

Figure 2.16 Fourier coefficients of the discrete transform viewed as corrupted estimate for the continuous Fourier transform: (a) $x(t)$ and Fourier transform $X(f)$, (b) unit amplitude window $w(t)$ and $W(f)$, (c) convolution of $x(t)$ and $w(f)$, (d) discrete sampling function, (e) convolution $x(t)$, $w(t)$, and $c(t)$, and (f) discrete bandwidth limited function based on (e). Source: Ref. [1].

The continuous frequency domain function shown in Fig. 2.16(e) can be made discrete if the time function is treated as one period of a periodic function. This forces both the time domain and frequency domain functions to be infinite in extent, periodic and discrete (Fig. 2.16(f)). *The discrete Fourier transform* is reversible mapping of N terms of the time function into N terms of the frequency function. Some problems are outlined later.

2.13.1 Leakage

Leakage is inherent in the Fourier analysis of any finite record of data. The record of the data is obtained by looking at the function for a period T and neglecting everything

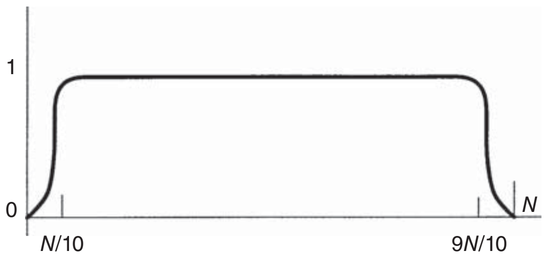

Figure 2.17 An extended data window. Source: [B1].

that happens before and after this period. The function may not be localized on the frequency axis and has side lobes (Fig. 2.8(b)). The objective is to localize the contribution of a given frequency by reducing the leakage through these side lobes. The usual approach is to apply a data window in the time domain, which has lower side lobes in the frequency domain, as compared to a rectangular data window. An extended cosine bell data window, called Tukey's interim data window, is shown in Fig. 2.17. A raised cosine wave is applied to the first and last 10% of the data, and a weight of unity is applied for the middle 90% of the data. A number of other types of windows that give more rapidly decreasing side lobes have been described in the literature. Some of the window types are as follows:

- Rectangular
- Triangular
- Cosine squared (hanning)
- Hamming
- Gaussian
- Dolph–Chebyshev

For periodic functions, the rectangular window results in zero spectral leakage and high spectral resolution. The rectangular window spans exactly one period, the zeros in the spectrum of the window coincide with all harmonics except one. This results in no spectral leakage under ideal conditions.

A window function often incorporated in spectrum analyzers is Hanning window.

$$W(t) = 0.5 - 0.5 \cos\frac{2\pi t}{T}, \quad \text{for} \qquad -0.5T < t < 0.5T \tag{2.92}$$

The function is easily generated from sinusoidal signals. The main lobe noise bandwidth is greater than that in a rectangular window. The highest side lobe is at −32 dB and side fall-off rate is −60 dB (see Fig. 2.18(a) and (b) for comparison of rectangular and Hanning windows).

The *Hamming* window function is

$$W(t) = 0.54 - 0.46 \cos\frac{2\pi t}{T}, \quad \text{for} \qquad -0.5T < t < 0.5T \tag{2.93}$$

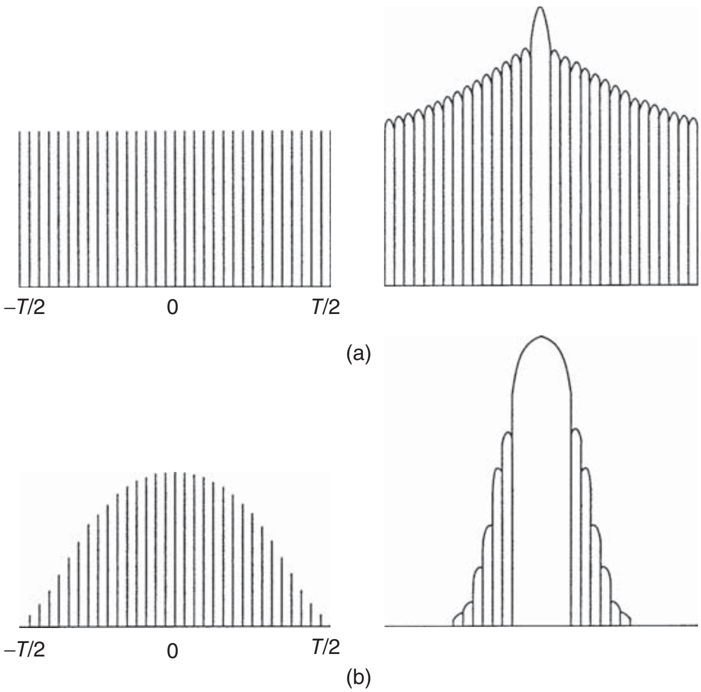

Figure 2.18 (a) Rectangular window and (b) hanning window.

2.13.2 Picket Fence Effect

An analogy between the output of fast Fourier transform (FFT) algorithm and a bank of band-pass filters is shown in Fig. 2.19. Each Fourier coefficient ideally acts as a filter having a rectangular response in the frequency domain. In practice, the response is of the type with side lobes. In Fig. 2.19, main lobes only have been plotted to represent output of FFT. The width of each lobe is proportional to the original record length.

When the signal being viewed is not one of these orthogonal frequencies, the picket pence effect becomes evident. The picket fence effect can reduce the amplitude of the signal in the spectral windows, when the signal being analyzed falls in between the orthogonal frequencies, say between the third and fourth harmonics. The signal will be experienced by both the third and fourth harmonic spectral windows, and in the worst case halfway between the computed harmonics. The signal is then reduced to 0.637 in both the spectral windows. Squaring this number, the peak power is reduced to 0.406.

By analyzing the data with a set of samples that are identically zero, the FFT algorithm can compute a set of coefficients with terms lying in between the original harmonics. As the width of the window is related solely to the record length, the width of these new spectral windows remains unchanged: that means a considerable overlap.